MOLECULES INVOLVED IN THE SPIDER, *CUPIENNIUS SALEI*, MECHANOTRANSDUCTION

by

Jessica Johnson

Submitted in partial fulfilment of the requirements
for the degree of Master of Science

at

Dalhousie University
Halifax, Nova Scotia
July 2019

TABLE OF CONTENTES

LIST OF TABLES

LIST OF FIGURES

ABSTRACT

The molecular mechanisms involved in mechanical senses such as touch and vibration have been studied for decades using a small number of model preparations in species facilitating genetic manipulation. Recent advances in molecular biology have allowed these studies to expand into wider variety of organisms and preparations. The strain detecting VS-3 slit sensillum of the spider, *Cupiennius salei,* is an important model because it contains large mechanosensory neurons that allow simultaneous intracellular recording during mechanical stimulation. Messenger RNA sequences encoding members of several putative mechanotransduction channel families have been found in spider transcriptomes. My aim was to discover if any of these molecules were involved in mechanotransduction, using in situ hybridization, pharmacological agents, and RNA interference. Taken together, my results indicate that Piezo protein is the strongest candidate for a VS-3 neuron mechanotransduction channel. However, it is possible that it functions together with an amiloride sensitive epithelial sodium channel.

LIST OF ABBREVIATIONS AND SYMBOLS USED

A/D	Analog to digital
Amil	Amiloride sensitive ion channel
ANC	Anterior neuron cluster
ANOVA	Analysis of variance
AP	Action potential
ASIC	Acid sensitive ion channels
ax	axons
BCIP	5-bromo-4-chloro-3-indolyl-phosphate-toluidine salt
BSA	Bovine serum albumin
C. salei	*Cupiennius salei*
CB	Central body
cDNA	Complementary deoxyribonucleic acid
CG	Cheliceral ganglion
CHAPS	3-[(3-Cholamidopropyl)dimethylammonio] -1-propanesulfonate
CNS	Central nervous system
CY-3	Cyanine-3 conjugated fluorescence dye
DAPI	4′,6-diamidino-2-phenylindole
DCL	Dorsal protocerebral cell layer
de	Dendrites
DEG	Epithelial sodium channel (ENaC) in Degenerin family
DEPC	Diethyl pyrocarbonate
df	Degrees of freedom
DMSO	Dimethyl sulfoxide
DNA	Deoxyribonucleic acid
DRG	Dorsal root ganglion
dsRNA	Double-strand ribonucleic acid

E	Electrical stimulation
EDTA	Ethylenediaminetetraacetic acid disodium salt dihydrate
ENaC	Epithelial sodium channel
eso	Esophagus
F	*F*-statistics a ratio of two variances
F	Forward polarity
GsMTx4	Grammostola Mechanotoxin #4
HEPES	4-(2-Hydroxyethyl)piperazine-1-ethanesulfonic acid
LG1-4	Leg ganglia 1-4
M	Mechanical stimulation
mec	mechanosensory abnormal
mORF	Main open reading frame
mRNA	Messenger ribonucleic acid
n	Number of experiments
NBT	Nitroblue Tetrazolium Chloride
NOMPC	NO mechanoreceptor potential C
O/N	Overnight
OG	Opisthosomal ganglia
ON	Optic neuropils
p	probability value of significance in statistics
PBS	Phosphate-Buffered Saline
PBST	0.1% Triton X-100 in PBS
PBT	0.1% Tween-20 in PBS
PCR	Polymerase Chain Reaction
PCL	Posterior cell layer
PPG	Pedipalpal ganglion
PPK	*Drosophila* ENaC channel pickpocket

R	Reverse polarity
RNA	Ribonucleic acid
RNAse	Ribonuclease
RR	Ruthenium Red
RT-PCR	Reverse transcription-polymerase chain reaction
RT-qPCR	Reverse transcription-Quantitative polymerase chain reaction
SD	Standard Deviation
SE	Standard Error
so	Soma
SSC	Saline Sodium Citrate
Sub.es	Subesophageal ganglion
Sup.es	Supraesophageal ganglion
t	measures the size of the difference relative to the variation in sample data.
TMC	Transmembrane channel-like protein
Tris	Tris(Hydroxymethyl)aminomethane
tRNA	Transfer ribonucleic acid
TRP	Transient receptor potential
TRPA	Transient receptor potential (ankyrin repeat)
TRPC	Transient receptor potential (canonical)
TRPM	Transient receptor potential (melastatin)
TRPML	Transient receptor potential (mucolipins)
TRPN	Transient receptor potential (NO mechanoreceptor potential C)
TRPP	Transient receptor potential (polycystic)
TRPV	Transient receptor potential (vanilloid)
TTX	Tetrodotoxin
VS-3	German “Vorderseite-3”, front side-3

ACKNOWLEDGEMENTS

I would like to express my very great appreciation to my supervisors, Dr. Päivi Torkkeli and Dr. Andrew French. They have provided me with unimaginable opportunities that have shaped me into the one I am, and have pushed me to my full potential. Their assistance, guidance, and patience were crucial for the development of this thesis.

I would like to thank Dr. Hongxia Liu for her guidance in molecular work especially in situ hybridization and RNAi and Dr. Ulli Höger for teaching me the electrophysiological experimentation using mechanical stimulation. Thank you both for taking the time to share your knowledge with me, provide assistance and friendship.

I would also like to extend thanks to Kajanan Sivapalan for his results from immunocytochemistry, locating the Piezo protein in *C. salei* central nervous system and Dr. Thomas Suchyna and Dr. Alexander Quinn for generously providing GsMTx4 and Yoda1, respectively. Thanks to Dr. Keram Pfeiffer who provided an excellent photograph of a spider for this thesis.

I also extend my appreciation and gratitude to the members of my supervisory committee – Dr. Younes Anini, Dr. Xianping Dong and Dr. Alexander Quinn, as well as my external examiner, Dr. Ian Meinertzhagen, and defence chair, Roger Croll. Thank you for your assistance and time that has made this possible.

Lastly, this research was supported and funded by the Nova Scotia Research and Innovation Graduate Scholarship, the DeWolfe Scholarship from the Dalhousie Medical Research Foundation, the Department of Physiology and Biophysics Graduate Scholarship and the Natural Sciences and Engineering Research Council of Canada.

CHAPTER 1. INTRODUCTION

1.1. Mechanotransduction

Mechanotransduction is the process of creating a biological response through the conversion of mechanical forces into electrochemical signals. The ability to respond to mechanical forces and displacements has great importance in all animals through diverse mechanisms, as they are all exposed to a range of external mechanical stimuli, including touch, sound, mechanical pain and internal mechanical forces such as proprioception and vascular tone (Paluch et al. 2015; Parpaite and Coste 2017). Mechanosensitive ion channels allow specialised sensory neurons to detect external mechanical stimuli such as touch and auditory signals very rapidly, within micro- to milliseconds (Nilius and Honoré 2012; Parpaite and Coste 2017). Opening of these ion channels allows ions to pass through, causing a depolarizing (Na^+ or Ca^{2+} influx) or hyperpolarizing (K^+ efflux) change in the membrane potential (Nilius and Honoré 2012).

Two basic models have been proposed for the gating of mechanosensitive ion channels. The bilayer model suggests that the lipid bilayer transmits the force directly to the mechanotransduction channel, while the tether model involves interaction of the channel with elastic filaments connected to the cytoskeleton, the extracellular matrix, or both (Nilius and Honoré 2012; Katta et al. 2015).

For an ion channel to be considered a mechanotransduction channel in a mechanosensory cell, four specific criteria have been defined (Katta et al. 2015). First, the channel must be expressed in the sensory cell responsible for mechanotransduction and localized in the correct position within the cell. This can be determined using in-situ

hybridization and immunocytochemistry. Second, the channel must be necessary for generating an electrical response to the mechanical stimuli. This is different from signal amplification, filtering or signalling that follows the initial response. Deletion of the channel should remove this response (Árnadóttir and Chalfie 2010; Katta et al. 2015).

The third criterion requires that when these channels are expressed in cultured cells or lipid bilayers, they should have similar properties as the native channels. These include ion selectivity and sensitivity to the same agonists and antagonists (Katta et al. 2015). The fourth criterion requires that the heterologously expressed channel must be activated by mechanical stimuli. This may be difficult to achieve experimentally, because specialized cellular and accessory structures that participate in mechanotransduction are probably eliminated from the system (Katta et al. 2015).

None of the eukaryotic ion channels that have been considered as mechanotransduction channels fulfill all these criteria. However, there is significant evidence for the roles of several ion channel families in the mechanotransduction of a variety of animal models and they are described below.

1.2. Mechanotransduction channels

1.2.1. DEG/ENaC/ASIC channels

The degenerin/epithelial sodium channel (DEG/ENaC) superfamily that also includes Acid Sensitive Ion Channels (ASIC) assemble as trimers to form amiloride sensitive Na^+ selective ion channels that play a variety of roles in Na^+ homeostasis (Kashlan and Kleyman 2011). Members of this family have been implicated in mechanotransduction by the nematode *Caenorhabditis elegans* gentle touch neurons

(O'Hagan et al. 2005; Árnadóttir and Chalfie 2010). Chalfie and Sulston (1981) screened *C. elegans* mutants that did not respond to gentle touch and found 16 *mec* (mechanosensory abnormal) genes. Two of them, *mec-4* and *mec-10* encoded homologous proteins to the mammalian ENaC channel and are believed to form the pore of the *C. elegans* mechanotransduction channel (Chalfie et al. 1993; O'Hagan et al. 2005).

MEC-4 and MEC-10 proteins have been localized in discrete puncta in the *C. elegans* touch neurons and their elimination makes the worms insensitive to gentle touch (O'Hagan et al. 2005; Cueva et al. 2007). Mechanical stimulation of intact *C. elegans* touch receptor cells caused rapid and transient activation of a Na^+-selective mechanotransduction current that could be blocked by amiloride and eliminated by *mec-4* null mutation (O'Hagan et al. 2005). When expressed in heterologous cells, the MEC-4 channels were also Na^+ selective and blocked by amiloride (O'Hagan et al. 2005). Therefore, MEC-4 meets three of the four criteria for mechanotransduction channels described above (Katta et al. 2015). However, when *mec-4* and *mec-10* genes were co-expressed in *Xenopus* oocytes, they formed Na^+-selective channels, but they did not activate in response to membrane stretch (Goodman et al. 2002), failing the fourth criterion (Katta et al. 2015). This may be due to the lack of associated components, which may directly or indirectly help to gate the channel.

Mammalian ASIC channels have been attractive candidates for possible mechanotransduction channels (Omerbasic et al. 2014). Studies performed on double and triple ASIC knockout mice, indicate that they modulate the mechanosensitivity of sensory neurons (Omerbasic et al. 2014). For instance, ASIC3 has been found in

mechanoreceptor endings including Meisnner's corpuscles, Merkel cells, and free nerve endings (Price et al. 2001). ASIC3 mutant mice have impaired vagal afferent sensitivity and they do not demonstrate secondary hyperalgesia, the physiological process responsible for pain sensitivity (Bielefeldt and Davis 2008; Walder et al. 2010). ENaC and ASIC channels have also been shown to contribute to the mechanotransduction in mammalian muscle spindles (Simon et al. 2010). However, they do not produce mechanically activated currents in heterologous systems (Simon et al. 2010).

1.2.2. TRP channels

Transient Receptor Potential (TRP) channels are activated by many different stimuli including light, odors, tastants, acids, temperature and auditory and mechanical stimuli (Liu and Montell 2015). The seven well-conserved TRP subfamilies consist of: the canonical TRPC that includes the first ever identified TRP channel in *Drosophila* photoreceptors, vanilloid activated TRPV, TRPM that includes the tumor suppressing melastatin protein, TRPA that has many ankyrin repeats near its N-terminal end, TRPN that includes the *Drosophila* NOMPC (NO Mechanoreceptor Potential C), and TRPP that is associated with the polycystic kidney disease, and TRPML that is associated to the neurodevelopmental mucolipidoisosis disease (Liu and Montell 2015). Activation of some TRP channels involves several steps while others are activated more rapidly. For example, the arthropod phototransduction cascade starts with light activation of rhodopsin and leads to opening of TRPC channels, Ca^{2+} influx and depolarization (Hardie 2014; Saari et al. 2017). On the other hand, activation of the TRP channels by changes in force, temperature or binding of a ligand, only involve single steps (Liu and Montell 2015). Most TRP channels are unselective cation channels, but two TRPM

channels are not permeable to Ca^{2+} or other divalent cations while some TRPV channels are very highly Ca^{2+} permeable (Owsianik et al. 2006).

Mechanical force has been proposed as a common strategy for activation of all TRP channels, even when the initial stimulus is not mechanical (Hardie 2014; Liu and Montell 2014). In arthropods, specific TRP channels, described below, have been clearly linked to mechanotransduction in primary mechanosensory cells.

NOMPC

The TRPN1 channel NOMPC has 23 flexible ankyrin repeat domains in its amino terminus that are believed to link the channel to the cytoskeleton and function as gating springs (Liang et al. 2013). NOMPC was first found in the adult *Drosophila* bristle hair neurons, specifically localized at the distal tips of the sensory cilia (Walker et al. 2000; Lee et al. 2010). It has later been found in several larval and adult *Drosophila* mechanoreceptors, proprioceptors and the auditory Johnston's organs and suggested to serve as a major component of mechanotransduction (Cheng et al. 2010; Lee et al. 2010; Effertz et al. 2011). A null mutation of NOMPC reduced the transient mechanotransduction current leaving a small sustained response in bristle hair neurons (Walker et al. 2000) and failed to eliminate the sound induced responses in Johnston's organ (Eberl et al. 2000) suggesting that other components are needed for mechanotransduction in these organs. However, NOMPC forms functional mechanotransduction channels in heterologous expression systems, providing further evidence for its role in mechanotransduction (Gong et al. 2013; Katta et al. 2015).

Nanchung-Inactive

Two TRPV proteins, Nanchung and Inactive have been shown to form heteromultimeric channels to mediate responses to sound stimuli in the neurons of *Drosophila* Johnston's organ (Kim et al. 2003; Gong et al. 2004). The channels are localized in the proximal part of sensory cilia, the Nanchung protein is only expressed when Inactive is present and vice versa (Gong et al. 2004). This proximal location is too far from the ciliary tips where external force is detected, and it has been suggested that another protein (probably NOMPC) propagates depolarization along the cilium toward the dendrite (Göpfert et al. 2006). Both Nanchung and Inactive have been claimed (not shown) to form homomultimeric channels that are activated in hypotonic solution in cell cultures (Kim et al. 2003; Gong et al. 2004), but this may be caused by intrinsic properties of the cells (Warren and Matheson 2018). Auditory Müller's organ of the desert locust *Schistocerca gregaria* revealed that Pymetrozine, a specific agonist of Nanchung-Inactive, produced inward currents that were similar in amplitude as the sound-evoked currents. While this agonist was present, additional sound stimuli did not evoke transduction currents (Warren and Matheson 2018).

Most recently, knockdown of the Nanchung or Inactive by RNA interference was shown to inhibit mechanically activated action potentials in the cockroach *Periplaneta americana*, tactile spine neuron while knockdown of NOMPC or Piezo had no effect (Hennenfent et al. 2019). These experiments demonstrate that Nanchung-Inactive could be, or form part of the mechanically activated channel in several insect mechanosensory neurons.

1.2.3. TMC proteins

In the vertebrate cochlea and vestibular system, sensory hair cells detect sound and spatial orientation, respectively (Fettiplace 2017). On the apical surface of each hair cell is the hair bundle consisting of interconnected stereocilia that contain the mechanotransduction channels. In the cochlea, sound-induced deflection of the basilar membrane results in movement of the hair bundles against the overlying tectorial membrane (Fettiplace 2017). Hair bundles are immersed in an extracellular fluid that has a high K^+ concentration and opening of the mechanotransduction channels leads to K^+ influx (Fettiplace 2017). The stereocilia connectors, tip links, are essential for mechanotransduction as their destruction eliminates transduction. The tip links become stretched during positive deflections, which opens the mechanotransduction channels, and they relax during negative deflections (Fettiplace 2017). Molecular structures of the tip links and multiple other proteins within the cilia have been identified in recent years (Qiu and Müller 2018). The molecular structure of the hair cell mechanotransduction channel pore has not yet been firmly identified but the best current candidate is the Transmembrane channel-like protein isoform-1 (TMC1) (Fettiplace 2017; Pan et al. 2018; Qiu and Müller 2018).

The *Tmc* family consists of eight genes in mammals (Keresztes et al. 2003) while invertebrates have only one or two (Holt et al. 2014). Mammalian *Tmc1* and *Tmc4* are expressed in the adult cochlea hair cells, whereas *Tmc2* is only expressed during early postnatal development (Kawashima et al. 2011; Scheffer et al. 2015). The TMC1 protein is concentrated in the tips of the stereocilia and its knockout causes hearing loss that can be rescued by TMC2 at earlier stages of development. Point mutations of the *Tmc1* also

alter the mechanotransduction channel conductance and Ca^{2+} permeability (Fettiplace 2017; Pan et al. 2018). TMC1 was shown to form a dimer and its pore region was recently revealed (Pan et al. 2018). However, TMC proteins have not yet been shown to form channels that respond to mechanical stimulation in heterologous expression systems, and therefore they do not meet all the criteria for mechanotransduction channel (Katta et al. 2015; Qiu and Müller 2018). Furthermore, these findings do not exclude the involvement of other proteins as components of the mechanotransduction channel (Pan et al. 2018).

1.2.4. Piezo proteins

Two proteins, Piezo1 and Piezo2, were discovered in 2010 in a mouse neuroblastoma cell line and shown to be activated by mechanical stimuli (Coste et al. 2010). Since then, orthologue proteins have been found in numerous eukaryotes and they have been shown to function as ion channels in both sensory cells, detecting stimuli such as touch and proprioception, and non-sensory cells where they are associated with diverse functions including cell volume regulation and blood flow (reviewed by Murthy 2017).

Piezos are very large proteins consisting of over 2,500 amino acids and more than 14 transmembrane domains with no homology to any other known proteins (Coste et al. 2010). The 3-dimensional structure of mouse Piezo1 has been resolved and it was shown to form homotrimers with a propeller-like architecture, containing three blades and a central ion conducting pore (Ge et al. 2015; Guo and MacKinnon 2017; Zhao et al. 2018). The channel is believed to be gated by changes in local curvature of the membrane (Guo and MacKinnon 2017).

While vertebrates have two Piezo proteins that share 50% identity, arthropods have only one that shares same identity with both vertebrate proteins (Coste et al. 2012; Kim et al. 2012). The vertebrate Piezo1 is found in non-neural tissues such as the bladder, kidney, lungs, and in the endothelial cells of the blood vessels (Parpaite and Coste 2017). Piezo2 is expressed mainly in neurons including a subset of somatosensory dorsal root ganglion (DRG) neurons, in the sensory neurons of the respiratory system and in the hair cells of the inner ear (Coste et al. 2010; Parpaite and Coste 2017). However, they are not involved in auditory transduction (Beurg and Fettiplace 2017). Lewis et al. (2017) have determined that heterologously expressed mouse Piezo1 and Piezo2 respond to a wide range of stimulus frequencies, which may be important for processing complex mechanical stimuli.

The *Drosophila* Piezo protein was shown to form mechanically activated channels in heterologous expression system (Coste et al. 2012). It had a significantly lower conductance than the mouse Piezo and it was insensitive to Ruthenium Red that blocks the mouse Piezo channels (Coste et al. 2012). The Piezo protein is located in all parts of many sensory and nonsensory neurons of *Drosophila* larvae and adults (Kim et al. 2012). Knockout flies had severe deficit in mechanical nociception while their responses to other types of noxious stimuli and touch were normal (Kim et al. 2012).

1.3. Arthropod mechanosensilla

Arthropod mechanosensilla are specialized sense organs that detect mechanical displacements, which can arise from external or internal sources. Examples of external mechanical stimuli are airborne vibrations and touch, while internal stimuli include joint rotations. Arthropod mechanosensilla can be divided into two groups (French 1988): The

Type I mechanosensilla contain bipolar sensory neurons whose distal dendrites are enclosed by dense material, giving the appearance of a sheath, tube or cap. This structure is connected to an external structure such as a hair or spine or to an internal structure as in chordotonal organs. Insect Type I mechanosensilla are subdivided to the hair sensilla, campaniform sensilla, and chordotonal sensilla. Type II mechanosensilla include multipolar sensory neurons, which usually connect to deeper, internal structures (French 1988).

The mechanosensilla perform a three-step process to detect mechanical stimuli (French 1988): 1) Coupling of the original mechanical stimulus to the membrane of the sensory neuron (e.g., deflection of a hair causes a deformation of the sensory dendrite). 2) Transduction, the displacement of the membrane causes a receptor current by opening of mechanically gated channels. 3) Encoding, where the graded receptor current causes a membrane potential change and usually one or more action potentials (French 2012).

In arthropod cuticular mechanosensilla, the sensory dendrite is attached to the cuticle and located in a large receptor lymph space surrounded by epithelium. In insects, this space has high K^+ concentration that creates a transepithelial potential difference and prompts a depolarization of the cell once the mechanotransduction channels open (Grünert and Gnatzy 1987; French 1988). Sensory cells are usually linked to accessory structures or materials that transmit the force to the mechanotransduction channels. Accessory structures may be involved in detecting the stimuli, filtering and/or amplifying mechanical signals.

1.4. *Cupiennius salei*

Spiders (order Aranea) are diverse group of predatory arthropods with over 48,000 species currently described (World Spider Catalogue 2019, https://wsc.nmbe.ch/). Recently revised taxonomy places *Cupiennius* in a genus of araneomorph spiders in the family of Trechaleidae (Piacentini and Ramírez 2019). *Cupiennius* spiders have eight circular eyes as shown in Figure 1.1 for *Cupiennius salei*, while other spiders may have oval or kidney-shaped eyes (Barth 2002). *Cupiennius* spiders are wandering or hunting spiders, found in Mexico, South America and Caribbean islands. They do not spin webs to catch their prey. Throughout the day they hide in plants with large leaves from where they either hunt, court for a partner or molt at night. They can also construct their own protective hiding spots by spinning together parts of the plant they retreat on. Females who carry an egg sac are particularly inclined to do this, and they even spin their retreat shut with a silk cover (Barth 2002).

When an insect prey creates vibrations at appropriate frequencies, the spider leaves its hiding place to catch it. In addition to the vibrations of a potential prey, spiders detect a broad spectrum of mechanical stimuli including delicate air currents and vibrations, and the slightest deformations of their exoskeleton and gentle touches. Spider courtship is a complex ritual, where both the male and female produce species specific vibratory signals to communicate with each other (Barth 2002).

Figure 1.1. Photograph of a male *C. salei.* (Courtesy of Dr. Keram Pfeiffer)

1.4.1. *C. salei* central nervous system

The central nervous system (CNS) of *C. salei* is in the anterior region of the body (prosoma) and consists of the supraesophageal and subesophageal ganglionic masses with the esophagus between them as shown in Figure 1.2A. The subesophageal ganglia include two anterior pedipalpal ganglia, eight leg ganglia, and the posterior abdominal (opisthosomal) ganglia (Figure 1.2B).

In the subesophageal ganglion are the nerves to the pedipalps and legs and their cell bodies are in the periphery ventrally and ventrolaterally (Figure 1.2B). The highly organized longitudinal and transverse layers of nerve fibers are in the interior of each ganglion (Babu and Barth 1984). Since these ganglia innervate the extremities, they contain many motor nerves and the mechanosensory and other sensory neurons from the periphery terminate here (Barth 2002).

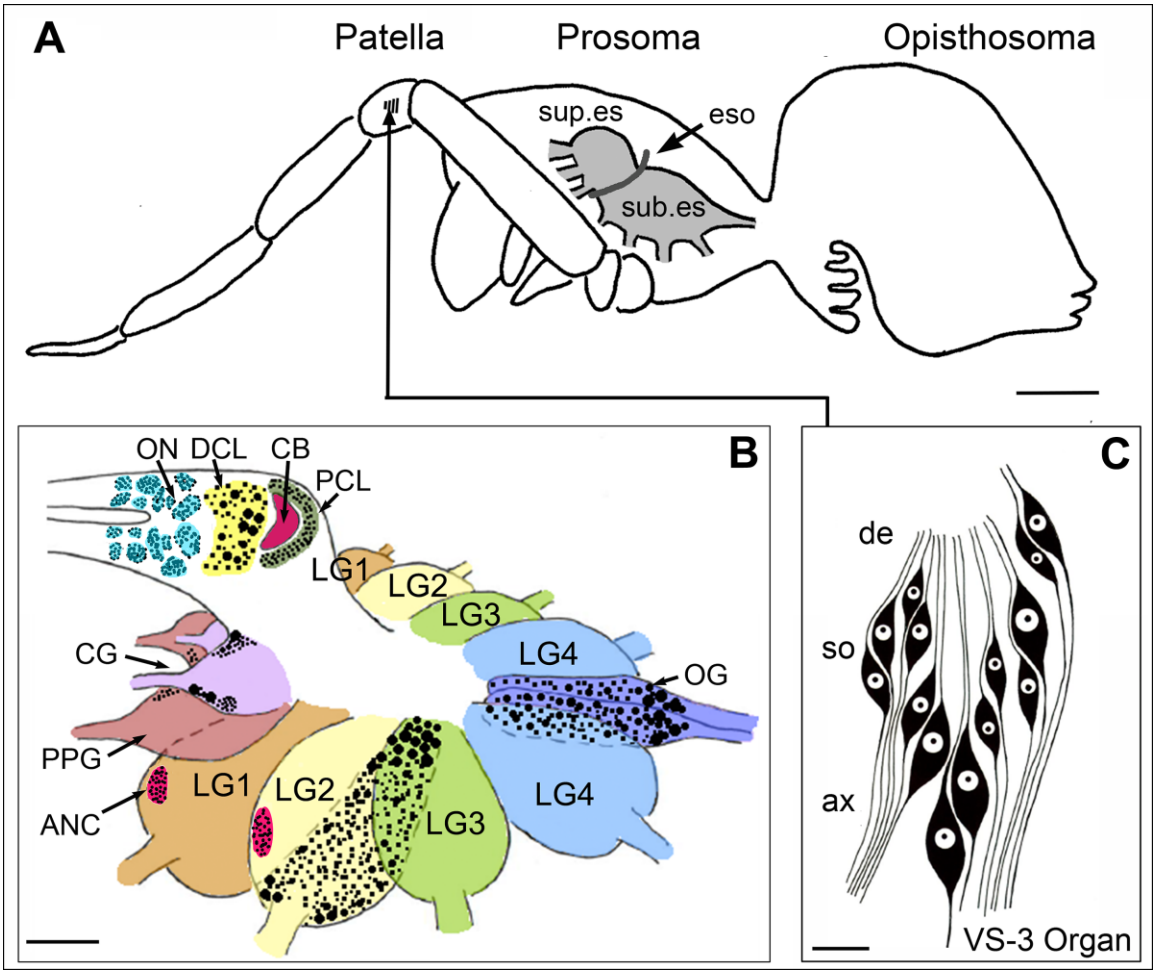

Figure 1.2. A schematic diagram showing the *C. salei* CNS and the VS-3 organ. (**A)** A diagram of the spider body and one leg is shown. The CNS is located within the prosoma and the esophagus (eso) separates the ventral subesophageal ganglion (sub.es) and the dorsal supraesophageal ganglion (sup.es). (**B)** The pedipalpal ganglion (PPG) is located in the Sup.eg. while the cheliceral ganglion (CG) and the four pairs of leg ganglia (LG1-4) are in the sub.eg. The somata of neurons in the sub.eg. are in the ventral cell layer (black dots in LG2 and OG). Anterior neuron clusters (ANC) are found in each leg ganglion. The sup.eg. consists of the CG, the posterior cell layer (PCL), the central body (CB), the dorsal protocerebral cell layer (DCL) and optic neuropils (ON). (**C)** The arrangement of bipolar mechanosensory neurons in the patellar VS-3 slit sensillum. Dendrites (de), somata (so) axons (ax) of seven pairs of neurons are shown. Scale bars A. 5 mm; B. 2 mm; C. 50 µm (Reproduced with permission from Fabian-Fine et al. 2017).

The supraoesophageal ganglion is the actual brain of the spider. It includes the cheliceral ganglia and three optic neuropils in each hemisphere and four pairs of optic nerves. The third optic neuropil is also called the central or arcuate body. The cheliceral ganglia gives rise to the nerves that innervate surrounding cheliceral muscles. The central body is made up of the dorsal and ventral lobes. Surrounding cell processes and fibre tracts end in the central body, with the most important tracts being those from the anterior median optic tract, the optic tract of the secondary eyes, and motor fibres from the suboesophageal ganglia (Babu and Barth 1984).

1.4.2. *C. salei* mechanosensilla

Spiders have several different types of mechanosensory organs, important for their survival. These include hairs that are sensitive to air flow (trichobothria), hairs that sense touch, and the slit sensilla that detect strains in cuticle (Barth 2004). The spider trichobothria hairs are analogous to insect filiform hairs. They have been used experimentally as models for sensors of airborne vibrations. They are very fine and extremely sensitive hairs that vary in length, and this allows detection of deflection frequencies ranging from 10 Hz to 960 Hz. This is important for the spider to identify the difference between a flying insect prey (>100 Hz) versus background air movement (<10 Hz) (Barth 2004).

Hair sensilla are the most common structures among the animal kingdom for detecting sensory stimuli such as touch, taste, odors and temperature. Spiders have thousands of tactile hairs all over their body. These hairs are especially important when the spider uses its front legs to explore its surroundings in the dark, as the hairs detect the pressure induced by obstacles. The slit sensilla are unique to arachnids (Barth 2002;

2004). Spider slit sensilla appear either as single slits, in pairs, or in groups that are arranged in an order that resembles a lyre (Barth 2002). They are named based on their locations in the spider legs and body (Barth and Libera 1970).

A unique feature of arachnid and crustacean mechanosensilla is that they receive extensive efferent innervation in the periphery (reviewed by Fabian-Fine et al. 2002). In *C. salei*, fine efferent fibers have been shown to form chemical synapses with the dendrites, soma and axons of the sensory neurons (Fabian-Fine et al. 1999; 2002). These efferents contain several transmitters that have been shown to modulate the excitability of the sensory neurons via multiple types of receptors (Panek et al. 2002; Widmer et al. 2005; Pfeiffer et al. 2009; Sukumar et al. 2018).

1.4.3. *C. salei* VS-3 slit-sensillum

The lyriform VS-3 organ of *C. salei* is located on the anteroventral side of the leg patella (VS = vordersite = anterior side, nomenclature of Barth and Libera 1970), as indicated in Figures 1.2A and 1.3B. The organ consists of seven to eight cuticular slits organized in a shape of a lyre. Each slit is innervated by a pair of bipolar neurons with spindle-shaped 20-100 µm long somata (Figure 1.2C). When electrical or mechanical step stimulation is applied, one neuron (Type A) in each pair responds by producing one or two action potentials, while the other neuron (Type B) responds with a train of action potentials (Seyfarth and French 1994). The Type A neuron has been shown to detect higher frequency stimuli than the Type B neuron (French et al. 2001)

Similar to insect cuticular mechanosensilla, the dendrites of spider slit sensilla are located in a receptor lymph space. However, there is no transepithelial potential in the spider slit sensilla and K^+ and Na^+ concentrations in the lymph space are similar to their

concentrations in hemolymph while the Ca^{2+} concentration is three times lower in the lymph space than in the hemolymph (Grünert and Gnatzy 1987).

Juusola et al. (1994) made the first recordings of mechanically activated action potentials and currents in the VS-3 neurons. Since then, several different approaches have been used to investigate the properties of the receptor current and the excitability of the neurons while they have been subjected to various pharmacological treatments (e.g., Höger et al. 1997; Gingl et al. 2004; Pfeiffer et al. 2009). The VS-3 neuron mechanically activated current is strongly Na^+ selective as expected based on the high Na^+ concentration in the receptor lymph space (Juusola et al. 1994; Höger et al. 1997). This current could be blocked by Gd^{3+} and by amiloride, both of which have been widely used to investigate mechanically activated channels in other preparations. Gd^{3+} effect was not specific since it also blocked voltage activated currents in the VS-3 neurons (Höger et al. 1997). The effect of the ENaC channel blocker amiloride on VS-3 neuron receptor current was very slow, taking about 1 hour until the current disappeared (Höger et al. 1997). The VS-3 neuron mechanotransduction channels were also shown to be sensitive to pH, opening more easily in acidic condition than neutral or alkaline pH (Höger and French 2002).

The single channel conductance of VS-3 neuron mechanotransduction channels was estimated by noise analysis to be 7.5 pS and the number of channels about 250 in each cell (Höger and French 1999). The receptor current occurs very locally at the distal dendrites and decays rapidly. However, the action potentials that are driven by voltage activated Na^+ channels, also initiate at the dendritic tips, near the site of

mechanotransduction and then propagate regeneratively along the 100-300 μm dendrites to the soma and then to the axons (Seyfarth et al. 1995; Gingl and French 2003).

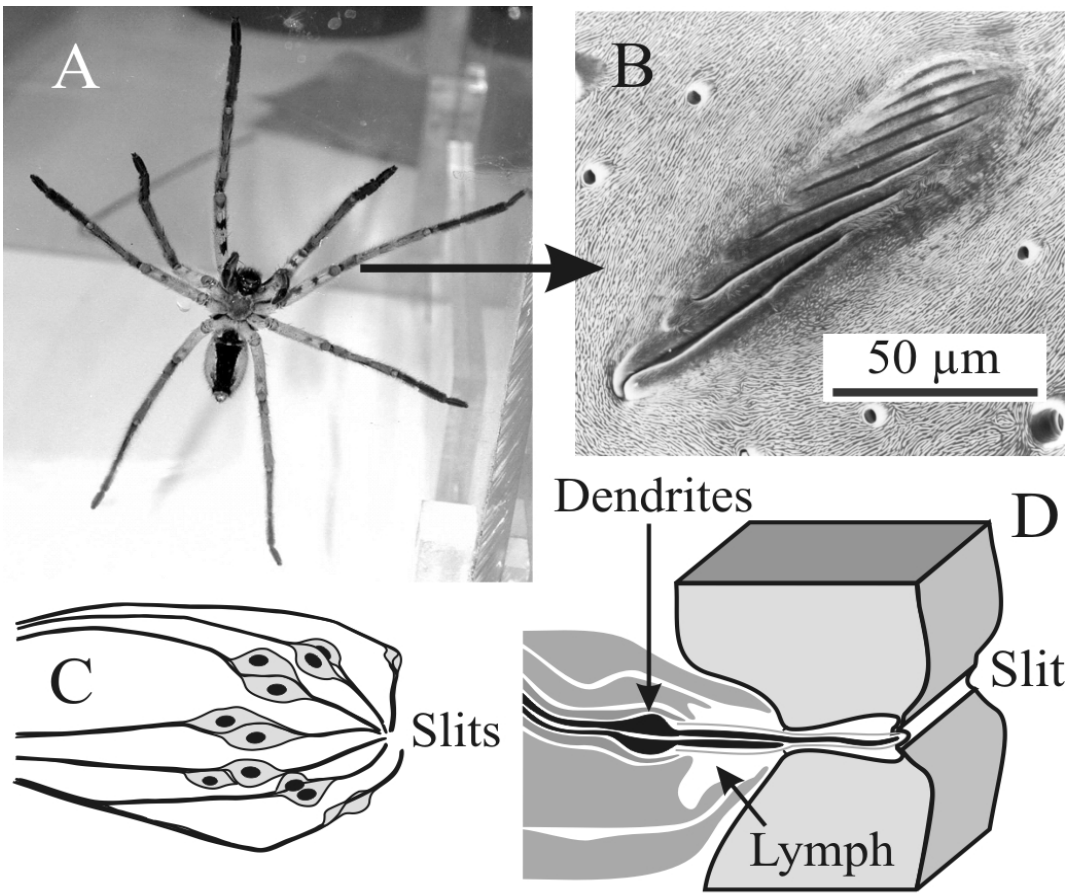

Figure 1.3. *C. salei* VS-3 slit sensillum **(A)** Adult male *C. salei* with arrow pointing from the location of the VS-3 organ on the patella. **(B)** Scanning electron micrograph of the slits on the exterior of the cuticle. **(C)** Depiction of the paired bipolar VS-3 neurons innervating the slits. Axons proceed proximally to the CNS**. (D)** Depiction showing the detail of slit innervation. Pairs of sensory dendrites are wrapped in three layers of supporting cells and the enlarged region of dendrites leads to the receptor lymph space. One dendrite of each pair enters the slit while the other terminates at the slit entrance. Both ends of the dendrites are surrounded by a thick cuticular sheath. Reused with permission from the authors (French and Torkkeli 2004).

1.4.4. *C. salei* transcriptome

During the past decade, deep mRNA sequencing has become a widely used method to investigate transcriptomes of tissues and cells and it provides a useful and

economical way of investigating various molecular mechanism in animal species that are not traditional model species with sequenced genomes. A transcriptome is defined as the complete set and quantity of RNA transcripts in a cell or tissue at the time when the RNA was extracted (Wang et al. 2009).

C. salei transcriptomes were created from total RNA extracted from their CNS and hypodermis tissues by Illumina sequencing in McGill University and Génome Québec Innovation Centre. The raw cDNA data consisted of >200 million random nucleotide sequences. This data has been used to assemble over 500 genes de novo using custom written software (French 2012). The *C. salei* gene sequences have been used to investigate evolutionary relationships of various molecules, to create probes for in-situ hybridization and RT-qPCR as well as manufacture custom made antibodies (Torkkeli et al. 2015; Liu et al. 2017; Fabian-Fine et al. 2017; Sukumar et al. 2018). They have provided valuable new data especially for determining the molecules involved in synaptic transmission. I used the transcriptome data in this thesis extensively to determine the proteins involved in mechanotransduction.

1.4.5. *C. salei* Piezo protein

The *C. salei* Piezo is a large protein with 2571 residues and a molecular weight of 295 kDa. A homology model of the spider Piezo amino terminal end that is believed to contain the pore region was a close match to the mouse Piezo1 structure (Figure 1.4, Zhao et al. 2018; Torkkeli et al. 2018). The *C. salei* Piezo shares 31% similarity with both the mouse Piezo1 and Piezo2 proteins and 32% similarity with the *Drosophila* Piezo.

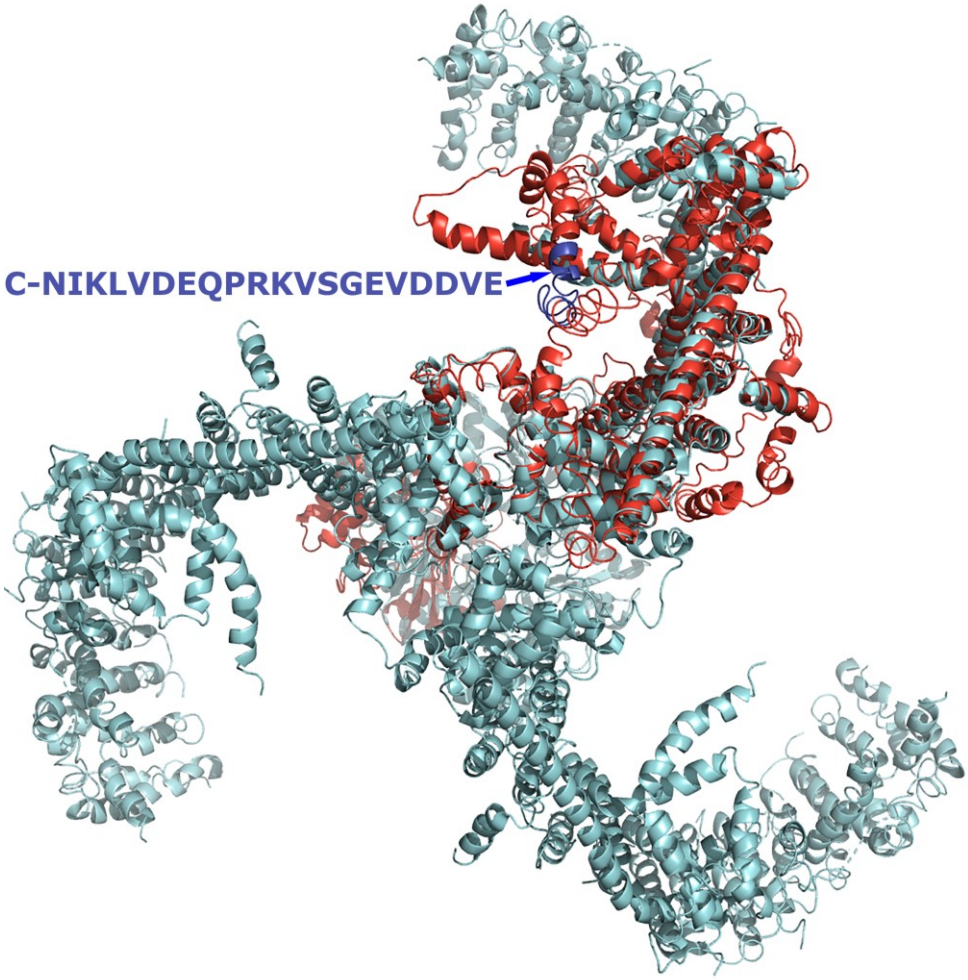

Figure 1.4. Cartoon model of the trimeric mouse Piezo1 (PDB5Z10, Zhao et al. 2018) viewed from top is shown as ribbon diagram (Blue). Homology model of the *C. salei* Piezo amino terminal end (residues 1265-2571) was created using the I-Tasser server and is shown in red aligned to one of the mouse Piezo1 subunits. Location of the residue that was used for antibody production is indicated (Courtesy of Dr. Torkkeli).

For my undergraduate honor's project, I tested two custom made polyclonal antibodies against the *C. salei* Piezo protein in immunocytochemistry and Western blot analysis. One of these antibodies found a specific band in Western blot at the expected molecular weight (Figure 1.5).

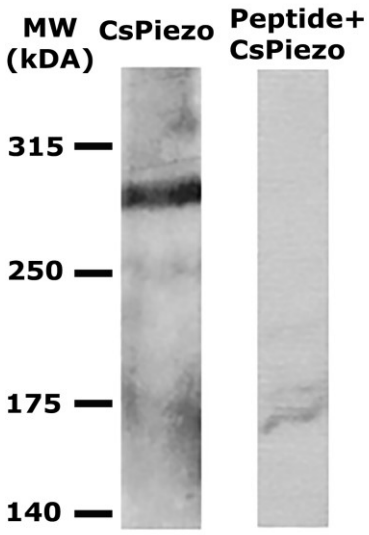

Figure 1.5. Western blot of the *C. salei* brain homogenate with an antibody against the Piezo antibody produced a specific band at 295 kDa. When the antibody was incubated 1 hour with 5-fold excess of the peptide used for immunization, there was no specific band.

In immunocytochemistry, the same Piezo antibody labeled strongly the VS-3 neuron dendrites, axons and leg nerve while the immunoreactivity in the soma was not nearly as strong (Figure 1.6). Double labeling experiments with a monoclonal antibody against *Drosophila* synaptic vesicle protein synapsin that labels the synaptic vesicles in the efferent nerves in spider hypodermis (Klagges et al. 1996; Fabian-Fine et al. 2002), revealed that the Piezo labeling was not in the efferent neurons, but specific for the VS-3 and other sensory neurons embedded in the hypodermis. Labeling of mechanosensory dendrites may indicate that the Piezo protein has a role in sensory mechanotransduction, but the widespread labeling of other parts of the neurons and the leg nerves suggests that this protein must also have other important functions.

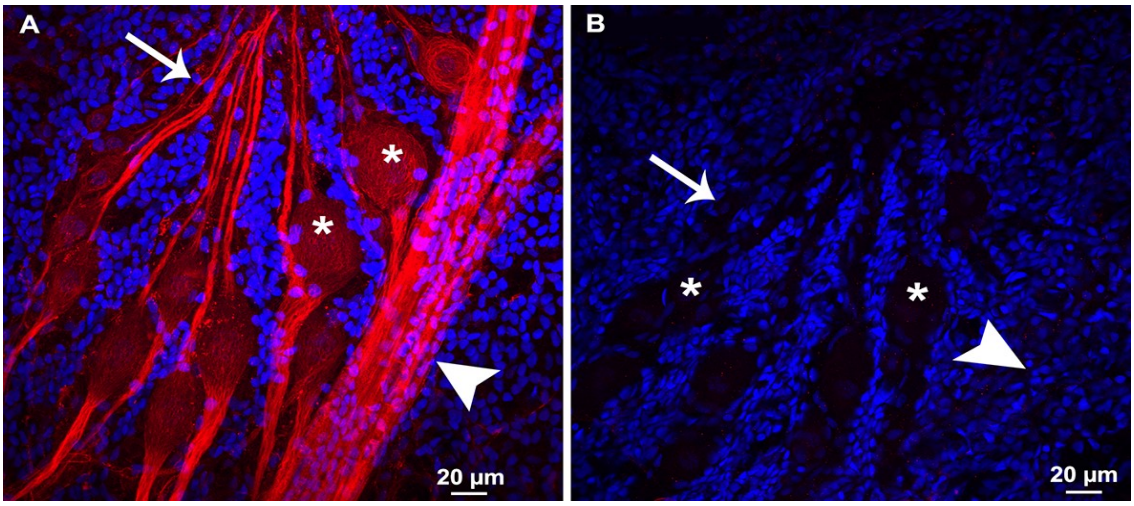

Figure 1.6. Immunocytochemistry with the *C. salei* Piezo antibody **(A)** A custom-made polyclonal antibody against the Piezo protein was tested by immunocytochemistry in whole-mount preparations of the spider patellar hypodermis with CY-3 (red) as the secondary antibody. Confocal images show strong red fluorescence at 1:2,000 concentration in VS-3 neuron dendrites (arrow), axons, around the cell body (*) and in the leg nerve (arrowhead). **(B)** When the Piezo antibody was incubated for 1 hour with 5-fold excess of the peptide used for immunization, there was no labeling in the hypodermis. DAPI (blue) was used as nuclear counterstain in both experiments.

1.5. Objectives

The major goal of this thesis was to investigate the molecules that may be involved in mechanotransduction in the *C. salei* VS-3 organ. Searches of the spider transcriptome revealed nine genes that are members of the gene families that have been identified as mechanotransduction channels in other preparations. Therefore, my first aim was to use in-situ hybridization to determine whether any of these genes are expressed in VS-3 neurons. The *Piezo* gene was one of the most likely candidates since the immunocytochemistry revealed strong labeling in mechanosensory neurons. However, this labeling was more widespread than expected for a mechanotransduction channel that should be located at the distal dendrites. Therefore, I investigated whether this gene is also expressed in other neurons using sections of the spider CNS. My second aim was to

determine if the VS-3 neuron mechanotransduction channels could be identified using pharmacological tools and electrophysiological experiments. For this, I tested the effects of two known inhibitors of mechanotransduction channels, Ruthenium Red and GsMTx4, on the VS-3 neuron receptor current and I also tested the effects of a specific Piezo1 agonist, Yoda1, on their excitability. The epithelial Na^+ channel blocker, amiloride has previously been shown to inhibit VS-3 neuron receptor current. Here, I tested the amiloride effects on the overall excitability of these neurons. My third aim was to determine whether it is possible to use RNA interference to knock down potential mechanotransduction channel genes in the spider cuticular preparations and to investigate these preparations using electrophysiology.

CHAPTER 2. MATERIALS AND METHODS

2.1. Experimental animals and dissection

Central American wandering spiders, *Cupiennius salei* (Keys), were maintained in the laboratory at room temperature (22°C ± 2°C) under a 13/11-hour light/dark cycle. Adult (≥10 months) male and female spiders were used in all experiments following protocols approved by the Dalhousie University Committee for Laboratory animals.

2.1.1. Dissection of the patella and VS-3 organ

For in-situ hybridization and electrophysiology, legs from adult spiders were autotomized and pinned on Sylgard (Dow Coring, Auburn, MI) coated dissection plates. For in-situ hybridization the dissection was performed in RNAse free phosphate buffered saline (PBS, Thermo Fisher, Mississauga, ON). For electrophysiology, spider saline containing 223 mM NaCl, 6.8 mM KCl, 8 mM $CaCl_2$, 5.1 mM $MgCl_2$ and 10 mM HEPES (4-(2-Hydroxyethyl)piperazine-1-ethanesulfonic acid), pH 7.8 (Höger et al. 1997), was used. The dissection was performed under a stereo microscope (Stemi 2000 Stereozoom, Carl Zeiss, Oberkochen, Germany) using a Fiber-Lite MI-150 High Intensity Illuminator (Dolan-Jenner Industries, Boxborough, MA). The patella and small parts of the femur and tibia were shaven, the leg was slit from the middle and the muscles on top of the VS-3 organ were carefully removed. For in-situ hybridization, the hypodermis, that holds the sensory neurons, was then partially lifted from the cuticle at the femoral joint, ensuring that the VS-3 organ was detached from the cuticle. This step ensured that at the end of the protocol, the entire hypodermis with intact VS-3 organ could be safely lifted from the cuticle. For electrophysiology, the patellar preparations

were used with the hypodermis attached to the cuticle. This ensured that the VS-3 neuron dendrites did not detach from the slits allowing recordings of responses to mechanical stimulation.

For in-situ hybridization, eight patellar preparations were transferred into 2 mL micro-centrifuge tubes containing 1 mL ice-cold 4% paraformaldehyde (Riedel de-Haen, Seelze, Germany) in PBS and fixed for 1 h. Shorter fixation times made the hypodermis fragile, caused the cells to detach easily and gave significant background staining. All incubation steps were performed at room temperature on a 2-dimensional rocker (BenchRocker™, Mandel Scientific, Guelph, ON) unless otherwise indicated. After fixation, the samples were rinsed 3 times for 5 min in PBST (0.1% Triton X-100 in PBS) and dehydrated through methanol (Fisher Scientific, Ottawa, ON) series: 25%, 50% and 75% methanol 5 min each and 100% methanol 3 times 5 min. Samples were stored in the final 100% methanol at -20°C for a minimum of one night and up to one month.

2.1.2. Central nervous system dissection

Spiders were first anaesthetized using carbon dioxide (CO_2) and their legs and fangs were removed using spring scissors (Fine Science Tools, Vancouver, BC). The spider torso was placed in a Petri dish and 3 mL of 4% paraformaldehyde was injected into the heart in the dorsal abdomen. Observations of fluid leaking from the leg joints indicated that the fixative perfused throughout the CNS. The abdomen was removed, and the cephalothorax was placed in a Sylgard coated Petri dish filled with PBS. With the ventral side upright, the cephalothorax was positioned for dissection using insect pins through 4 to 5 leg remnants. A razor blade was used to cut the soft tissue surrounding the sternum. The mouthparts were detached and discarded. This caused the sternum to come

loose, and it was lifted off to visualize the CNS mass. Spring scissors were used to cut the dorsally attached muscle and connective tissue, until the CNS mass became detached from the remaining cephalothorax.

All muscle and connective tissue surrounding the CNS was removed. The esophagus, which runs between the sub- and supraesophageal ganglia, was carefully removed. The CNS mass was then fixed overnight in 15 mL of 4% paraformaldehyde at 4°C on a rocker. Following fixation, the brain was washed three times for 5 min each in PBS at room temperature on a rocker. The brain was dehydrated in a methanol series as described for the VS-3 organ above and stored in 100% methanol at -20°C a minimum of one night and up to one month.

2.2. RNA probe construction for in-situ hybridization

Putative mechanotransduction channel genes were identified from transcriptomes prepared from *C. salei* leg hypodermis and CNS using methods described earlier for other genes in detail (French 2012; Torkkeli et al. 2015). Primers for sequences listed in Appendix 1 were custom-designed and purchased from Integrated DNA Technologies (IDT, Coralville, IA). They were amplified using polymerase chain reaction (PCR) following the method described by Liu et al. (2017). Digoxigenin-labeled antisense and sense RNA probes were then transcribed in-vitro from previously obtained cloning plasmids or spider hypodermis cDNA using T7 polymerase (Roche Diagnostics, Laval, QC; Torkkeli et al. 2015) following protocols given by the manufacturer. Agarose gel electrophoresis was used to confirm the probe quality, and probes were stored at -80°C until needed.

2.3. In-situ hybridization protocol for patellar samples

The in-situ hybridization protocol was adapted from Liu et al. (2017). All experiments were performed under RNAse-free conditions until the hybridization stage was completed. To maintain these conditions, disposable RNase free plasticware was used and nondisposable plasticware, glassware and dissection tools were treated with RNaseZap (Sigma, Oakville, ON) followed by multiple rinses with RNAse free water. RNAse free water was made in the laboratory using DEPC-treatment: 0.1% diethyl pyrocarbonate (DEP001; Bioshop, Burlington, ON) was added to double distilled water, shaken vigorously, incubated at 37°C for 12 h followed by autoclaving for 15 min to remove any traces of DEPC. All reagents were either purchased RNAse free or prepared using RNAse free water. Nitrile gloves were worn during the complete protocol.

During the first day of in-situ hybridization, the patellar samples containing VS-3 organ were removed from the freezer and rehydrated through the methanol series: 75%, 50% and 25% methanol 5 min each and 3 times 5 min in PBST. The samples were then divided into different tubes and labeled according to the probes that were used. For each test 8-10 legs were used, but some of these were lost during the long protocol. The total numbers for successful samples for each probe and hybridization and staining temperatures are listed in Table 2.1.

Table 2.1. In-situ hybridization conditions

Name	Number of preparations		Hybridization temperature	Staining reaction
	Antisense	Sense		
Piezo	17	7	63°C	37°C 4 h
Tmc-7	12	8	61°C, 63°C	37°C 4 h
Tmc-5	9	5	61°C, 63°C	37°C 4 h
Amil-1	14	12	60°C, 63°C	37°C 4 h, O/N RT
Amil-2	17	13	63°C	37°C 3 h, O/N RT
Trp-1	8	8	60°C, 63°C	37°C 4 h
Trp-2	9	6	60°C, 63°C	37°C 4 h
Deg-1	11	7	60°C, 63°C	37°C 4 h
Deg-2	13	12	60°C, 63°C	37°C 4 h

Probe names as in Appendix 1. O/N = overnight; RT = room temperature

The samples were incubated in 1 µg/mL Proteinase-K (Roche, 03 115 887 001) in PBST for 20 minutes to permeabilize the tissue followed by three 5 min PBST rinses. The samples were then incubated 20 min in 4% paraformaldehyde to stop the Proteinase-K reaction and washed again twice in PBST. To stop the RNAse activity the samples were then treated with 0.1% active DEPC in PBST twice for 15 min and then washed three times for 5 min in PBST. Before the hybridization, the samples were equilibrated at room temperature in 50% hybridization buffer (Table 2.2) in PBST for 5 min, then in 100% hybridization buffer for 5 min and finally 2 h in a new 100% hybridization buffer in a Techne HB-1D hybridization oven in a rotating tube (Cole Parmer, Vernon Hills, IL) at the specific temperature for each probe (Table 2.1).

Shortly before the hybridization, 200 ng/mL of the probe was added to the hybridization solution in a microcentrifuge tube and placed in a heating block (Fisher) at 80°C for 5 min and then immediately moved on ice for 5 min. This step straightens the long probes (615-828 bases) used in these experiments. The samples were then incubated in the hybridization solution containing the probe for overnight in the hybridization oven in the temperatures shown in Table 2.1. Once the probe for *Piezo* was shown to produce very strong staining, it was used as a positive control for experiments with other probes. For each gene, antisense and sense (control) probes were tested simultaneously.

Table 2.2. Hybridization solution

Solution	**Stock**	**15 mL**
Blocking Buffer (2 %) (see below)	10 %	3 mL
50% Formamide (Bioshop FOR001)	100 %	7.5 mL
5 X Saline Sodium Citrate, SSC (Thermo Fisher AM9765)	20 X	3.75 mL
100 µg/mL Heparin (Sigma H3393)	50 mg/mL	30 µL
0.1% Triton X-100 (Sigma T8787)	10%	150 µL
0.1% CHAPS (Bioshop CHA003)	10%	150 µL
5 mM EDTA (Sigma E5134)	500 mM	150 µL
100 µg/mL Yeast tRNA (Roche 10109495001)	100 mg/mL	15 µL
100 µg/mL Boiled Salmon Sperm DNA (Thermo Fisher 15632011)	10 mg/mL	150 µL
DEPC H_2O		Filled to 15 mL

10% Blocking buffer: Blocking regent (Roche 11 096 176 001) was dissolved in maleic acid buffer (100 mM Maleic acid; 150 mM NaCl, pH 7.5 with NaOH) final concentration of 10% dissolved by heating to 65°C. Aliquots were stored in -20°C;

CHAPS: 3-[(3-Cholamidopropyl)dimethylammonio]-1-propanesulfonate;

EDTA; Ethylenediaminetetraacetic acid disodium salt dihydrate.

2.3.1 Post hybridization washes

After in-situ hybridization was completed, double distilled water was used to prepare reagents. Following the hybridization, the samples were washed in a series of washing buffers (Table 2.3), in the hybridization oven at 66°C. First washing buffer was used once for 20 min, followed by three 20 min washes in second washing buffer, and in the end three 20 min washes in the third washing buffer. The tissue was then washed three times with PBST for 5 min each.

Table 2.3. Post hybridization washing buffers

Washing buffer 1	**Washing buffer 2**	**Washing buffer 3**
50% formamide	2 X SSC	0.2X SSC
5 X SSC	0.1% CHAPS	0.1% CHAPS
0.1 % CHAPS		
ddH_2O	ddH_2O	ddH_2O

2.3.2 Immunohistochemical detection

Blocking solution was prepared by dissolving Western blocking reagent (Roche 11 921 673 001) in 0.1% Tween-20 (Amresco, Solon, OH) in PBS. The samples were incubated in this solution for 2 h to block unspecific labeling followed by overnight incubation in the antibody (anti-digoxigenin-AP Fab fragments, Roche, 11 093 274 910) at 1:8,000 dilution in the blocking solution at 4°C on a rocker.

The next day, the samples were washed three times 10 min with 0.1% Tween-20 in PBS (PBT), then twice 5 min in freshly prepared pre-developing buffer consisting of 100 mM of Tris buffer (pH 9.8), 100 mM NaCl, 0.1% Tween-20 and 50 mM $MgCl_2$. The

developing buffer to visualize the alkaline phosphatase was prepared freshly and consisted of 100 mM Tris buffer, pH 9.8, 100 mM NaCl, 0.1% Tween-20, 5% polyvinyl alcohol (Sigma), 0.5% NBT (Nitroblue Tetrazolium Chloride, Bioshop, NBT001) and 0.375% BCIP (5-bromo-4-chloro-3-indolyl-phosphate-toluidine salt, Bioshop, BCI201). Samples were placed in the hybridization oven in the developing buffer and checked every hour to determine the progress of blue/purple staining. In few cases, the reaction was left to continue overnight at room temperature. The reaction times and temperatures are listed in Table 2.1.

Once staining was complete, the preparations were washed with PBS and placed in a PBS filled Sylgard-lined dish for dissection. At this point, the femoral and tibial joints were removed, and the hypodermis was lifted from the patella and placed in 1-2 drops of 70% glycerol (BDH, Dubai, UAE) in PBS on a superfrost plus microscope slide and a #1 micro cover glass was placed carefully on top. The samples were left overnight at room temperature after which the cover glass was secured in place using nail polish. The sections were observed with a compound microscope (Olympus BH-2, Richmond Hill, ON) and photographed using digital camera (MU500; AmScope, Irvine, CA). The photographs were processed in Adobe Photoshop CC 5 (Adobe Systems, San Jose, CA).

2.4. Central nervous system embedding, sectioning and in-situ hybridization

The CNS samples stored in 100% methanol in the -20°C freezer were dehydrated using a similar methanol series as described above for the patellar preparations. The brain was then embedded in a gelatin-bovine serum albumin (BSA) medium (Levin 2004; von Trotha et al. 2014; Fabian-Fine et al. 2017). This medium was prepared by heating 440 mg gelatin (300 bloom; Sigma) in 100 mL PBS to 60°C and stirring for one hour. Once

the solution cooled to room temperature, 27 g of BSA (Sigma A9418) was added and stirred until the mixture was completely dissolved. Aliquots were stored at -20°C until needed. To embed the tissue, aliquots were thawed, and the brain was equilibrated in the mixture for 5 minutes at room temperature. In the fume hood, the brain was placed in a plastic mold that was treated with RNaseZap. Gelatin-BSA mixture was supplemented with 6.47% formaldehyde and 0.075% glutaraldehyde and poured into the mold to immerse the brain. The block was left to solidify in room temperature for 5 to 10 minutes and then kept in a RNaseZap treated Tupperware container with a small amount of RNase free water at 4°C 4 to 10 days. The block was then sectioned using a Leica VT-1000S vibratome (Leica Biosystems, Wetzlar, Germany). 30 µm sections were collected in Netwell mesh bottom inserts (Electron Microscopy Sciences, Hatfield, PA) placed in a sterile 12-well cell culture dish filled with PBS. Sections were washed three times in PBST.

The in-situ hybridization protocol was similar to that described for patellar preparations above and used before for the spider CNS (Fabian-Fine et al. 2017). For the hybridization and antibody incubations steps, the meshwell inserts were placed on custom made plexiglass molds that required significantly smaller amounts of reagents than the cell culture dishes. Before the dye reaction, the sections were lifted onto microscope slides, let dry at 37°C, and then outlined by Pap Pen liquid blocker (Ted Pella, Redding, CA). The slides were placed on a custom-made slide holder that protected the developing reaction from light. The pre-developing and developing buffers were applied directly to the slides and the liquid blocker prevented leakage. The slide holder was placed in 37°C oven (Isotemp, Fisher) until the dye reaction was complete. Slides were then washed in

PBS three times and then covered with #1 coverslips mounted with a custom made gelatin/glycerol mounting media. Once solidified, the coverslips were secured with nail polish and the sections were observed and photographed as explained for the patellar preparations.

2.5. Electrophysiology

2.5.1. Experimental preparation

The cuticular preparation was mounted using beeswax into a custom-made preparation holder that consisted of a Falcon culture dish that had a longitudinal hole through the center, allowing access to both the outer and inner surfaces of the organ (Figures 2.1 and 2.2). The VS-3 organ was positioned in the middle of the hole, laid flat and secured on a holder on a gas-driven vibration isolation table (Technical Manufacturing, Peabody, MA). Neurons were visualized under brightfield optics using an upright compound microscope (Axioskop 2 FS Plus, Carl Zeiss), with Epiplan X10 and Achroplan X40 water-immersion objectives.

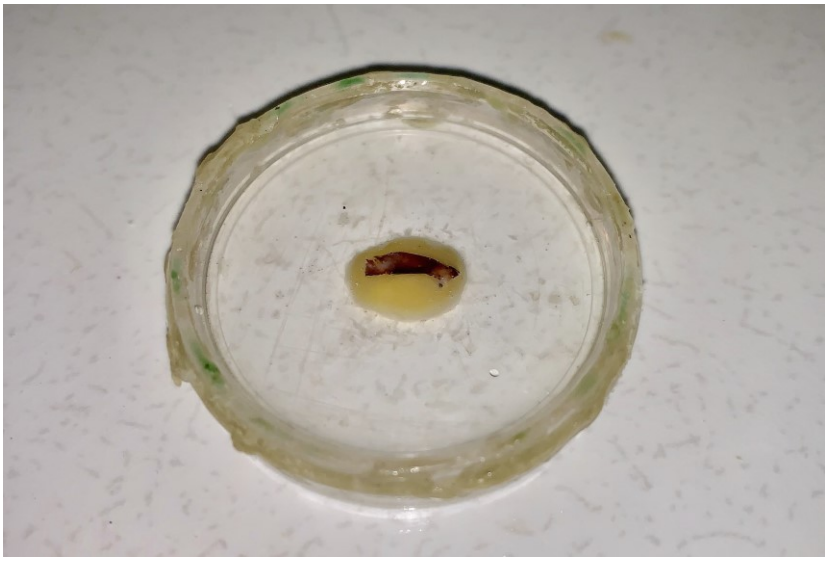

Figure 2.1. The VS-3 organ preparation for electrophysiology. The organ was secured on preparation holder using beeswax and filled with spider saline. The slits are located underneath the preparation and are accessible for mechanical stimulator while the neurons are facing up and accessible for the intracellular electrode. The preparation holder was mounted onto the experimental apparatus so that the femur, on the right, was oriented closest to and parallel to the microelectrode.

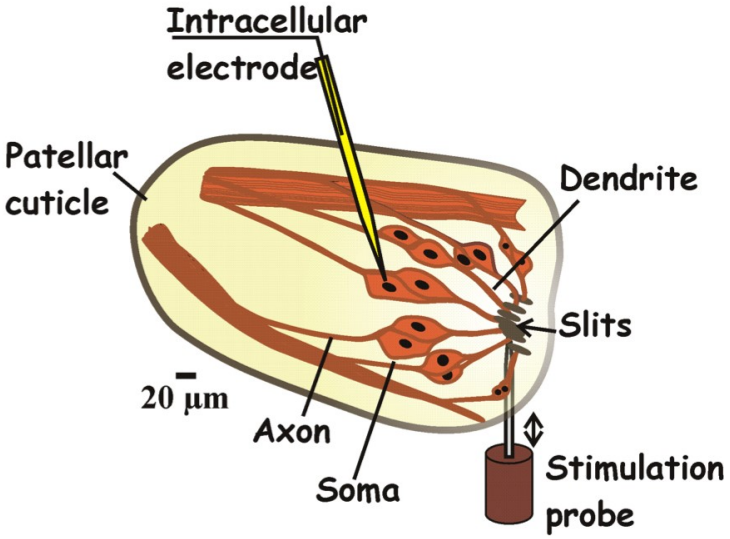

Figure 2.2. Experimental setup for the VS-3 organ. The mechanical stimulation probe was positioned underneath the slits. The intracellular electrode impaled the neurons to electrically stimulate and record cellular activity. The axons, somata and dendrites for the seven pairs of VS-3 neurons are shown as well as the underlying patellar cuticle. Modified from Panek et al. 2008.

2.5.2. Intracellular recording and mechanical stimulation

A P-2000 laser micropipette puller (Sutter Instrument, Novato, CA) was used to pull sharp microelectrodes from borosilicate glass with an outer diameter of 1 mm and inner diameter of 0.58 mm (World Precision Instruments, Sarasota, FL). The electrodes were filled with 3 M KCl and they had resistances between 40 and 80 MΩ in solution. The neuronal cell bodies were approached using a PatchStar micromanipulator (Scientifica, Uckfield, UK). and impaled by high-frequency oscillation ("buzzing").

In order to mechanically stimulate the slit-sense organ, a custom-made glass probe was positioned under the slits (Juusola et al. 1994, Höger et al. 1997). The glass probe was made using 1.5 mm outer diameter and 0.86 mm inner diameter borosilicate glass (A-M Systems, Everett, WA). The glass was pulled using the laser puller. The glass was then fire polished and melted until a glass bead of ~50 μm diameter was formed using a microforge (Narishige Scientific Instruments, Tokyo, Japan). The glass probe was then mounted on the holder of a P-841.10 piezoelectric stimulator driven by an E-505.00 LVPZT amplifier (Physik Instrumente, Auburn, MA). The stimulator was mounted on a three-dimensional micromanipulator (SD instruments, San Diego, CA) to easily position the probe tip underneath the VS-3 slits. The rise time of the step stimulus was 0.3 ms.

Recordings were made in discontinuous single-electrode current- or voltage-clamp mode using the SEC-10L amplifier (NPI electronic, Tamm, Germany) as described before (Torkkeli and French 1994; Sekizawa et al. 1999). All electrophysiological experiments were controlled by custom-written software (courtesy of Dr. Andrew French). Switching frequencies of about 20 kHz and a duty cycle of 1/2 (current passing/voltage recording) were used in all current-clamp experiments. For voltage-

clamp, 40 kHz switching frequency was used. The computer drove current, voltage, and mechanical stimulator signals via 12-bit to digital to analog (D/A) converters, while electrode current, membrane potential and stimulator position were recorded via 16-bit analog to digital (A/D) converters (National Instruments, Austin, TX). The membrane potential was low-pass filtered at 33.3 kHz and the current signal by 3.3 kHz by the voltage-clamp amplifier. Prior to performing voltage-clamp experiments, the inward Na^+-currents were blocked by 1 μM tetrodotoxin (TTX, see below). The preparations were superfused by spider saline.

2.5.3. Ion channel blockers and an activator

Ion channel blockers were initially diluted at high concentrations in double distilled H_2O unless otherwise indicted, aliquoted and frozen and then diluted to spider saline shortly before each experiment. They were applied to the bath via narrow tubing and replaced the bath solution completely. In all voltage-clamp experiments, 1 μM TTX with citric acid buffer (Sigma T5651) was used to block voltage gated Na^+ channels. Within 15 minutes, the VS-3 neurons stopped firing action potentials and mechanically induced receptor currents could be recorded. Ion channel antagonists that were tested were: Ruthenium Red (EMD Millipore 557450) used at 10 μM final concentration, synthetic D-amino acid form analog of GsMTx4, generously provided by Thomas Suchyna (University of Buffalo, NY), was used at 5 μM concentration, Amiloride hydrochloride hydrate (Sigma A7410) was initially dissolved at 100 mM concentration in dimethyl sulfoxide (DMSO, Sigma D8418) and used in final concentration of 1 mM in spider saline. Yoda1 (Cayman chemicals 21904, generously provided by Dr. T. Alexander Quinn) was tested at 25 μM concentration.

2.6. RNA interference

RNA interference pathway is initiated by Dicer enzyme that cleaves long double stranded RNA (dsRNA) into small about 21 long nucleotide sequences called small interfering RNA (siRNA). These breakdown products bind to the RNA-induced silencing complex, which then silences matching mRNA by degradation and blocking translation.

2.6.1. Construction of double stranded RNA

To construct dsRNA, reverse transcription (RT)-PCR was first performed using total RNA extracted from the spider CNS, and oligo $d(T)_{23}VN$ primers with ProtoScript II reverse transcriptase (New England BioLabs, Whitby, ON) using a previously described protocol (French et al. 2015). The cDNA was used in PCRs to amplify the template *Piezo* DNA using Q5 High-Fidelity DNA Polymerase (New England BioLabs). The primers

(Forward TAATACGACTCACTATAGGGGCAATGGAGTAGACTTCAAACTGCTG

Reverse TAATACGACTCACTATAGGGAGCACTCTATCCACGTATGGCATATC) used for the target DNA region of *Piezo* were tailed with the T7 promoter sequence TAATACGACTCACTATAGGG at their 5' end. The GenElute Gel Extraction Kit (Sigma) was used to purify the PCR products and the MEGAscript RNAi kit (Ambion, Burlington, ON) was used to synthesize dsRNA, following the instructions provided by the manufacturer. An agarose gel was run to confirm the quality of dsRNA and spectrophotometry was used to determine the concentration.

2.6.2. Tissue culture and processing

Sterile methods, tools and reagents were used throughout these experiments. Spider legs were autotomized as described above and prepared for dissection by manual cleaning. The patellar VS-3 organs were then dissected, ensuring that the hypodermis remained attached to the cuticle. Once dissected, each VS-3 organ was transferred into 2 mL of sterile spider saline supplemented with 20 µL of penicillin-streptomycin (Gibco, Grand Island, NY) and incubated for 3 h, on a rocker at room temperature.

Further processing of the tissue was done on a clean bench (The Baker Company, Sanford, ME). The patellae were transferred individually into wells of a 48-well cell culture plates with 200 µL of L-15 medium (Thermo Fisher) with 4 µg of the *Piezo* dsRNA. Control preparations were prepared otherwise in similar manner, but they lacked the dsRNA. The culture dish was sealed with sterile parafilm and placed in a tightly sealed sterile container in an incubator at 22.4°C (Sanyo, Osaka, Japan). The next day, 67 µL of L-15 media and 30 µL of fetal bovine serum (FBS, Hyclone, South Logan, UT) were added to each sample.

I performed electrophysiological experiments one, two and three days after preparations were exposed to dsRNA. Most of these experiments were done blind – I did not know if I had a control or a dsRNA treated sample until after the experiments were completed. Electrophysiological experiments were done while the preparations were in spider saline. Both electrical and mechanical stimulation were used under current clamp conditions.

2.7. Statistical analysis

Descriptive statistics were used to gather information including the means, standard deviation and standard errors for the data from electrophysiological experiments using Microsoft Excel software (Microsoft Canada Inc., Mississauga, ON). Bar graphs were initially created on Excel and processed using Adobe Illustrator. All data was tested for normality using the d'Agostino-Pearson test (Contchart Software 2019, https://contchart.com/goodness-of-fit.aspx). The VassarStats website was used for statistical analyses (Lowry 2019, http://vassarstats.net/) to test if any of the changes were statistically significant. If the data were normally distributed, I used the t-test for paired samples and one-way analysis of variance (ANOVA) for multiple samples. If the data were not normally distributed nonparametric tests were used. All tests are indicated in the results section. In the figures, statistical significances are indicated by asterisks: $*p \leq 0.05$, $**p \leq 0.01$, $***p \leq 0.001$.

CHAPTER 3. RESULTS

3.1. Putative mechanotransduction channels in *C. salei* transcriptomes

The relative abundances of transcribed mRNA for each putative mechanotransduction channel sequence was estimated by searching the transcriptome data for matches to the main open reading frame (mORF) as explained in detail earlier (French 2012; Torkkeli et al. 2015). The total counts were normalized by mORF length and expressed as abundance relative to the actin transcript. The relative abundances of each nine putative mechanotransduction channels in the hypodermis and CNS are shown in Figure 3.1.

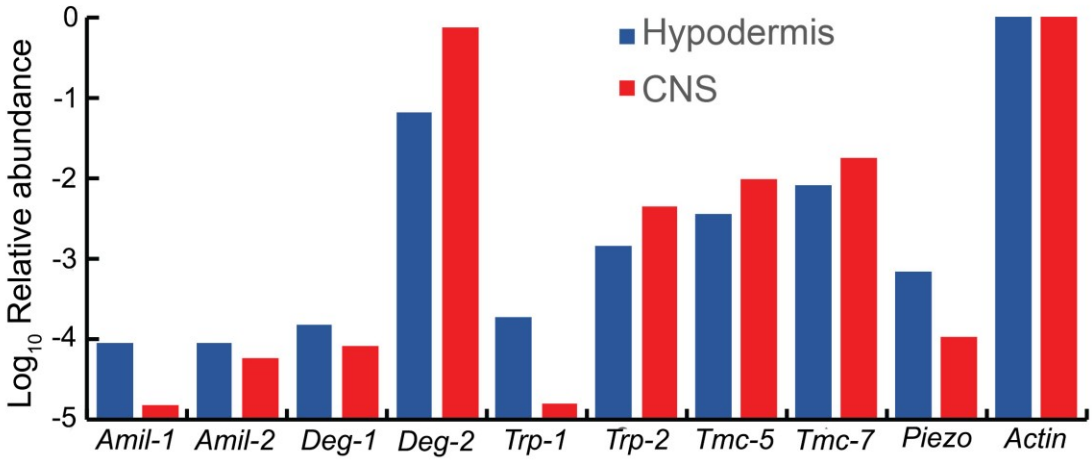

Figure 3.1. Relative abundances of putative mechanotransduction channel transcripts in the *C. salei* hypodermis and CNS transcriptomes. The data were obtained by counting total reads in the transcriptome libraries with at least 90 consecutive identical nucleotides to the reading frame of each gene, then normalizing by reading frame length. Abundances in hypodermis are indicated in blue while those in the CNS are indicated in red. The scale is logarithmic. Accession numbers and sequence nomenclature are shown in Appendix 1.

All sequences were found in both transcriptomes although the relative abundances of *Amil-1* and *Trp-1* were very low in the CNS. The most abundant transcript was the

Deg-2 in both transcriptomes and abundances of *Tmc-5* and *Tmc-7* channels and *Trp-2* were also relatively high. Both the CNS and hypodermis tissues that were used to create the transcriptomes contained neurons and glial cells, but some muscle tissue was also present and some of these transcripts may originate from muscle tissue.

3.2. In-situ hybridization

Expression of the putative mechanotransduction channel genes was investigated in whole-mount preparations of *C. salei* patellar hypodermis using in-situ hybridization with the probes listed in Appendix 1. The probe for *Piezo* was also tested on vibratome sections of the subesophageal ganglion. Each probe was initially tested using a hybridization temperature of 63°C that provided high stringency and the dye reaction was done at 37°C for 4 hours. If there was no, or faint, staining, the probe was re-tested at lower stringency using temperatures of 60-61°C, and in some cases the dye reaction was allowed to run overnight at room temperature to detect low abundance mRNA. For each experiment, 8-10 patellar preparations were used, but some of these were lost during the long protocol.

3.2.1. Expression of four genes in the DEG/ENaC/ASIC channel family

C. salei transcriptome searches found four transcripts that were homologous to *C. elegans* degenerins and the *Drosophila* ENaC channel pickpocket (PPK, Adams et al. 1998). They code proteins with molecular weights of 53-63 kDa. These sequences were named based on their closest homologues in GenBank as amiloride sensitive channels 1 and 2 (*Amil-1* and *Amil-2*) and degenerin 1 and 2 (*Deg-1* and *Deg-2*).

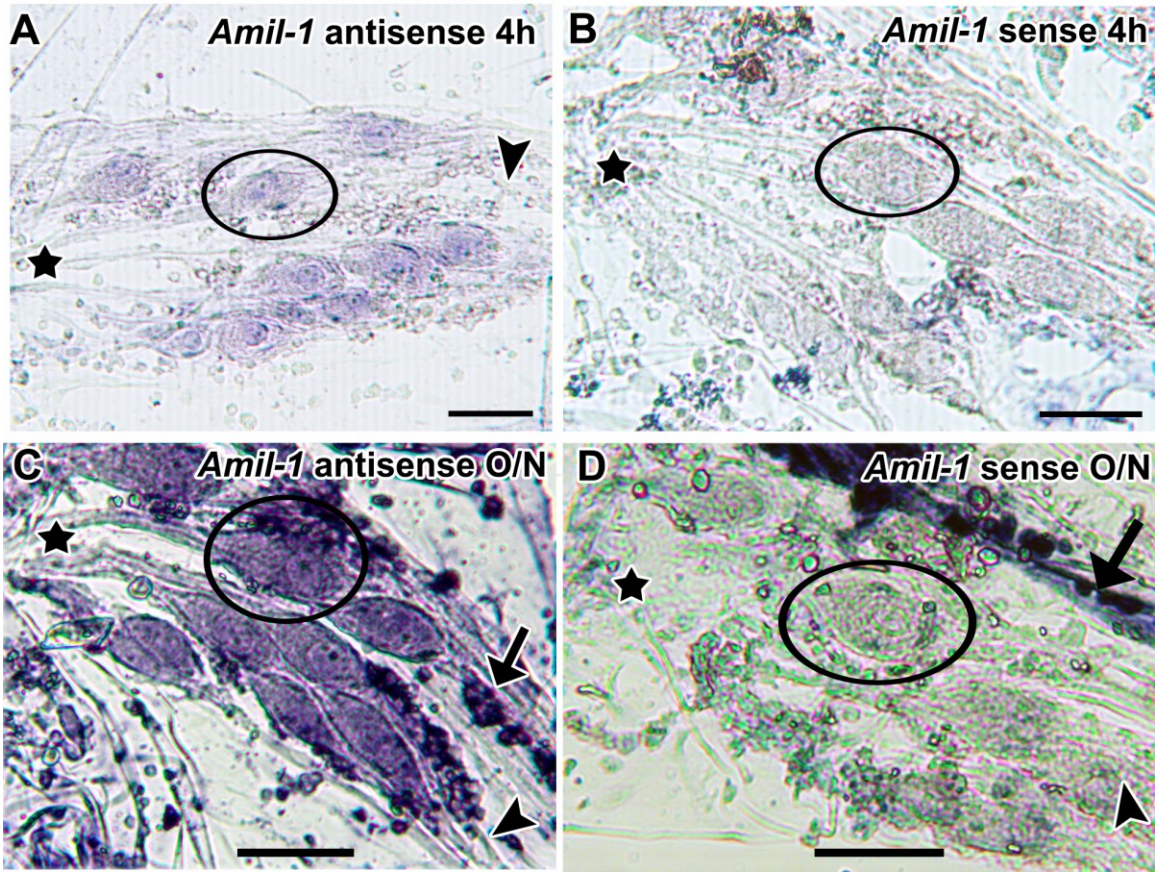

Figure 3.2. In-situ hybridization using the *Amil-1* probes. **(A)** Hybridization temperature of 60°C with the antisense probe and four-hour dye reaction produced faint labeling in the somata of VS-3 neurons. **(B)** The control (sense) probe did not produce any signal under the same conditions as in A. **(C)** Overnight (O/N) dye reaction and 63°C hybridization temperature produced strong labeling in the VS-3 neurons and the surrounding glial cells. Clusters of strongly labeled pigment cells are indicated with an arrow. **(D)** The sense probe did not produce any labeling in the VS-3 neurons or glial cells but some of the pigment cells were stained at the same conditions as in C. In each image, stars indicate the location of the dendrites, arrowheads point to axonal region and one soma is circled. Scale bars 50 µm in all images.

Amil-1 antisense probe produced faint staining when hybridization was done either at 63°C or 60°C (Figure 3.2A) after a dye reaction of four hours. When the experiment was done at 63°C and the dye reaction continued overnight, the VS-3 neurons were strongly labeled (Figure 3.2C). The glial cells that enwrap the VS-3 neurons and the pigment cells were also labeled. The control (sense) probe did not produce any labeling

in the VS-3 neurons or glial cells, although pigment cells were labeled after overnight dye reaction (Figure 3.2B and D).

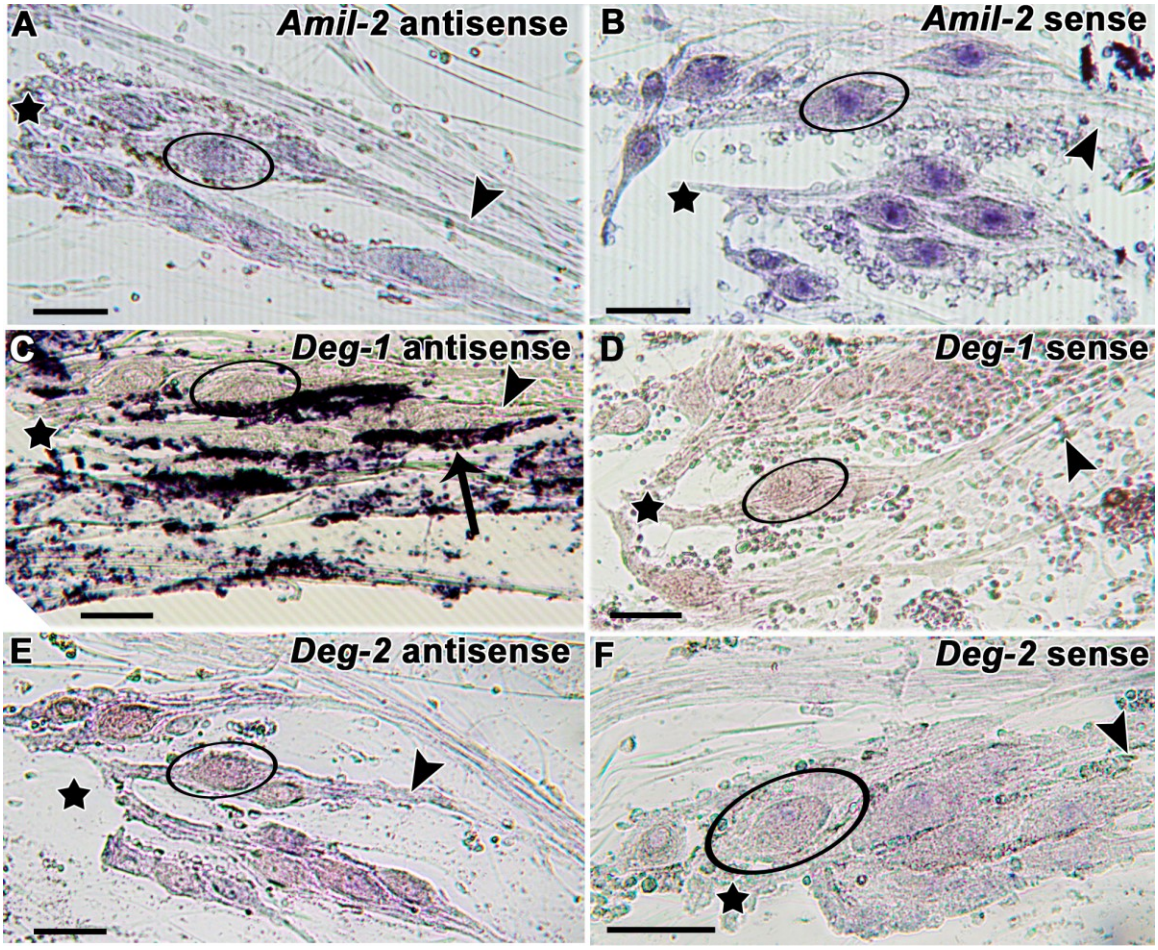

Figure 3.3. In-situ hybridization using probes for three ENaC channels. **(A)** Antisense probe for *Amil-2* at hybridization temperature of 60°C and four-hour dye reaction did not produce any signal in the VS-3 neurons. **(B)** *Amil-2* sense probe under the same conditions as in A labeled the nuclei of VS-3 neurons. **(C)** *Deg-1* antisense probe at 63°C hybridization temperature and 4-hour dye reaction did not produce any labeling on the VS-3 neurons, but the pigment cells were very strongly labeled in this preparation. **(D)** *Deg-1* sense probe did not produce labeling under the same conditions as in C. **(E)** and **(F)** *Deg-2* antisense or sense probes did not produce any signal at 63°C after 4-hour dye reactions. In each image, stars indicate the location of the dendrites, arrowheads point to axonal region and one soma is circled. Scale bars 50 µm in all images.

Hybridization temperature of 60°C and 4-hour dye reaction with antisense probe for *Amil-2* did not produce any labeling in VS-3 neurons while the sense probe labeled

the VS-3 neuron nuclei (Figure 3.3A and B). When preparations were incubated at 63°C and the dye reaction was continued for overnight, the antisense probe still did not produce any signal, but the sense probe labeled the cells even more strongly (data not shown). This result suggests that the sense probe was binding to DNA.

Antisense or sense probes for *Deg-1* (Figure 3.3C and D) or *Deg-2* (Figure 3.3E and F) did not produce any signal in the VS-3 neurons at 63°C hybridization temperature after 4 hour or overnight dye reaction. Some of these experiments were done using shorter fixation time than recommended and this resulted in strong labeling in the pigment cells (Figure 3.3C). When the same probes were tested at 60°C, there was more background labeling, but still no specific signal in the VS-3 neurons (data not shown).

3.2.2. Expression of two genes coding TRP channels

The *C. salei Trp-1* codes a protein that has a molecular weight of 190 kDa. Its closest homologues are the insect NOMPC channels. The *C. salei Trp-2* codes a smaller protein (89 kDa) that is closest to the canonical TRPC channels. At 63°C hybridization temperature, the antisense probe for *Trp-1* labeled the nuclear region of the VS-3 neurons and faint labeling in the same region was also visible when the sense probe was used (Figure 3.4A and B). When the hybridization temperature was lowered to 60°C, both the sense and antisense probes produced labeling all over the hypodermis indicating that the stringency for these probes was not adequate. The *Trp-2* antisense or sense probe (Figure 3.4C and D) did not produce any labeling in the VS-3 neurons under any conditions tested.

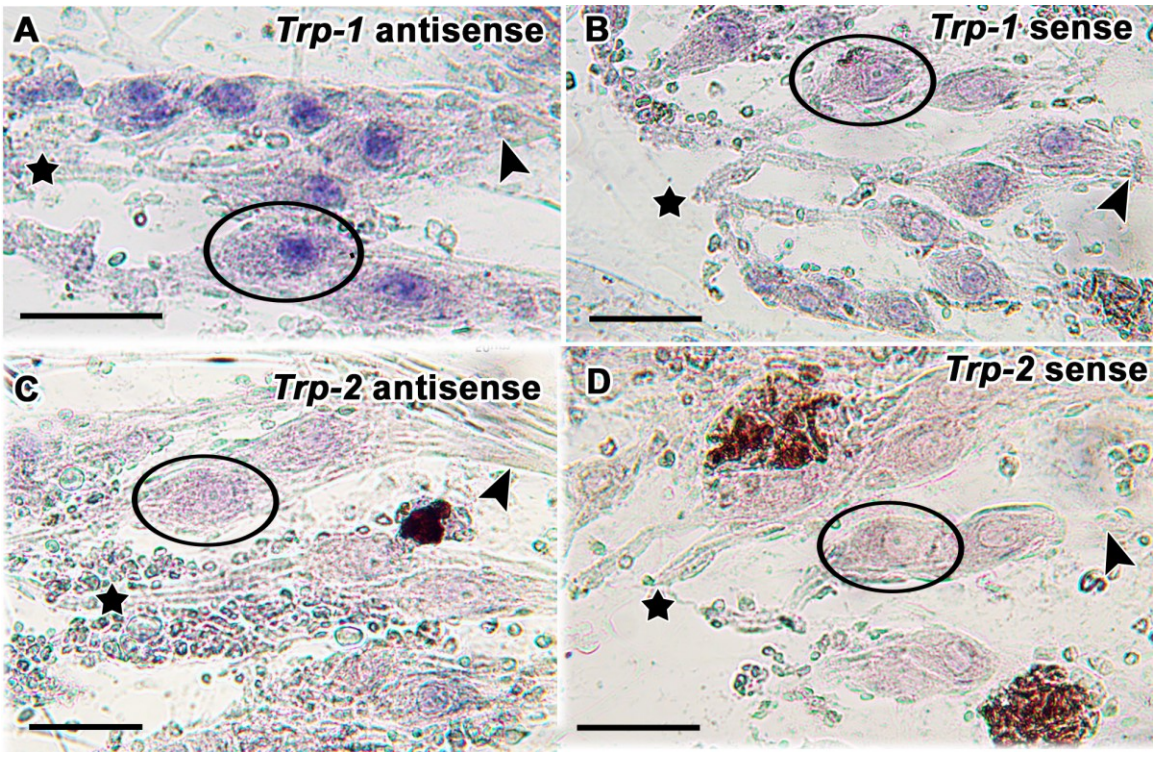

Figure 3.4. In-situ hybridization for *Trp* mRNA at 63°C and 4-hour dye reaction. **(A)** The *Trp-1* antisense probe produced labeling in the nuclear area of the VS-3 neurons. **(B)** The sense probe did not produce any signal in the VS-3 neurons. **(C)** and **(D)** No labeling was detected with the antisense or sense probes for *Trp-2*. In all images, asterisks indicate the dendritic region, arrowheads the axonal region and one soma of a VS-3 neuron is circled. Scale bars 50 µm in all images.

3.2.3. Expression of two genes coding TMC channels

The two *C. salei* transcripts that were found to be homologous to the transmembrane channel-like (TMC) proteins were named *Tmc-5* and *Tmc-7* based on their closest homologues in GenBank. They code proteins with molecular weights of 97 kDa (TMC-5) and 98 kDa (TMC-7). Antisense and sense probes for each transcript were tested at 63°C (Figure 3.5) and 61°C (data not shown) with dye incubation time of four hours. At 63°C there was no signal with either probe, although some background labeling was seen in pigment cells. When the stringency was reduced with lower hybridization

temperature, all cells were faintly labeled with all four probes, clearly indicating unspecific labeling.

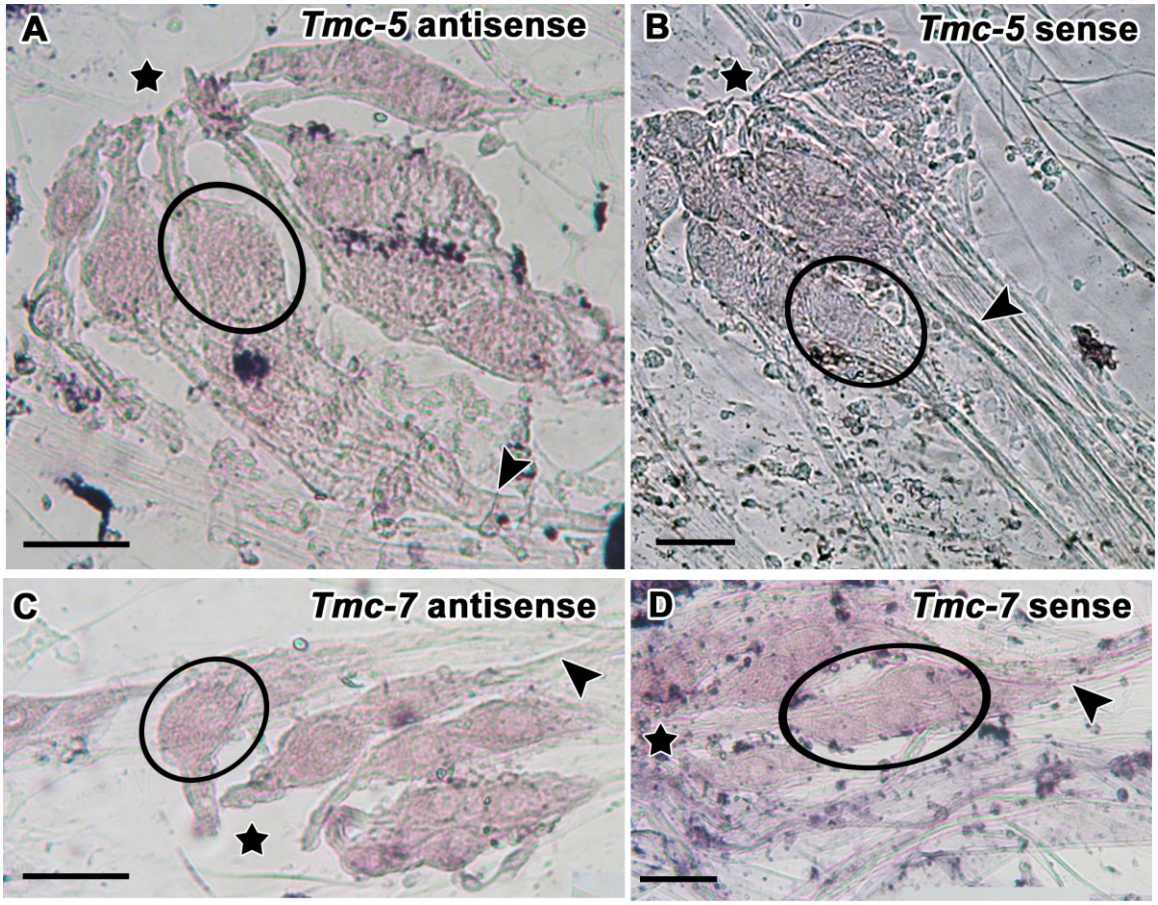

Figure 3.5. In-situ hybridization results for *Tmc* channels. Neither the antisense **(A)** or sense **(B)** probe for *Tmc-5* produced any signal in VS-3 neurons or other cells in the patellar hypodermis when the hybridization temperature was 63°C and dye reaction was done for 4 hours at 37°C. Under similar conditions the results with antisense **(C)** and sense **(D)** probes for *Tmc-7* were also negative. Stars indicate dendritic region, arrowheads axonal region and in each image one soma of a VS-3 neuron is circled. Scale bars 50 µm in all images.

3.2.4. Expression of *Piezo* in the *C. sale*i hypodermis and CNS

As explained in the Introduction, the custom-made antibody for Piezo protein labeled the VS-3 neurons very strongly, especially the dendritic and axonal regions. In

addition, the leg nerves were strongly labeled. These results suggest that even if Piezo protein would be the mechanotransduction channel in VS-3 neurons, it must also have other functions in the VS-3, and probably also in other neurons. To determine the extent of *Piezo* mRNA expression, cross sections of the subesophageal ganglion were investigated in addition to the patellar hypodermis. All experiments were done using 63°C hybridization temperature and 2-4-hour dye reaction at 37°C. The VS-3 neurons were very strongly and specifically labeled after only two hours in the dye reaction, indicating that *Piezo* is prominently expressed in these neurons (Figure 3.6A). There was no labeling when the sense probe was used (Figure 3.6B).

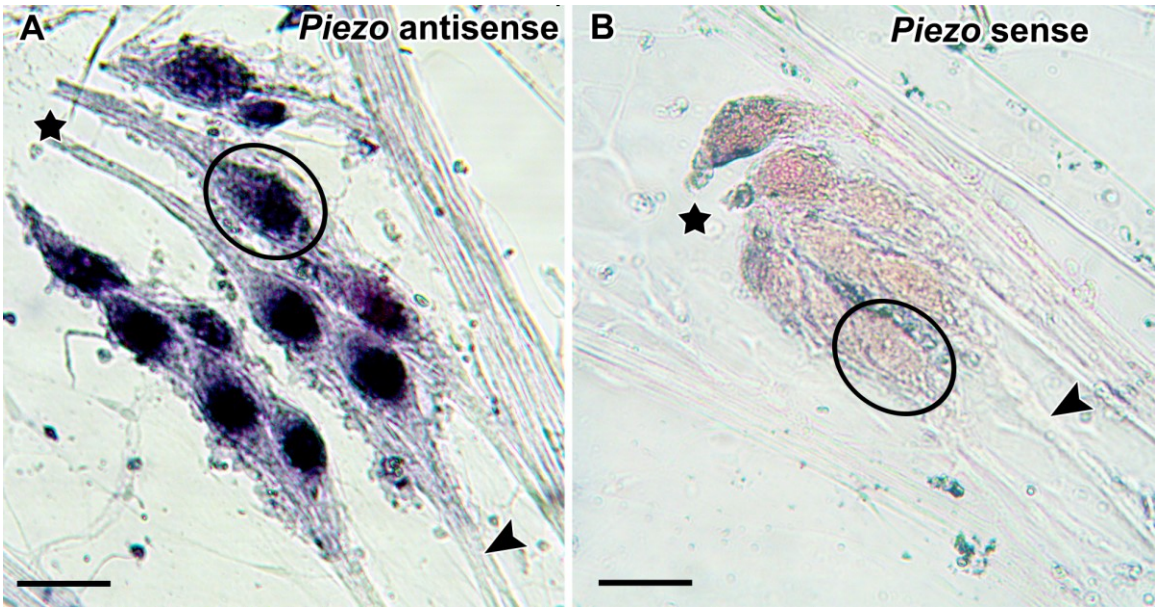

Figure 3.6. In-situ hybridization of VS-3 organ for *Piezo*. **(A)** Antisense probe produced a very strong signal in the VS-3 neuron somata at hybridization temperature of 63°C and 4-hour dye reaction in 37°C. **(B)** The sense probe did not produce any labeling under similar conditions. Stars indicate the dendritic region, arrowheads points to axonal region and one VS-3 cell soma is circled in both images. Scale bars are 50 µm in both images.

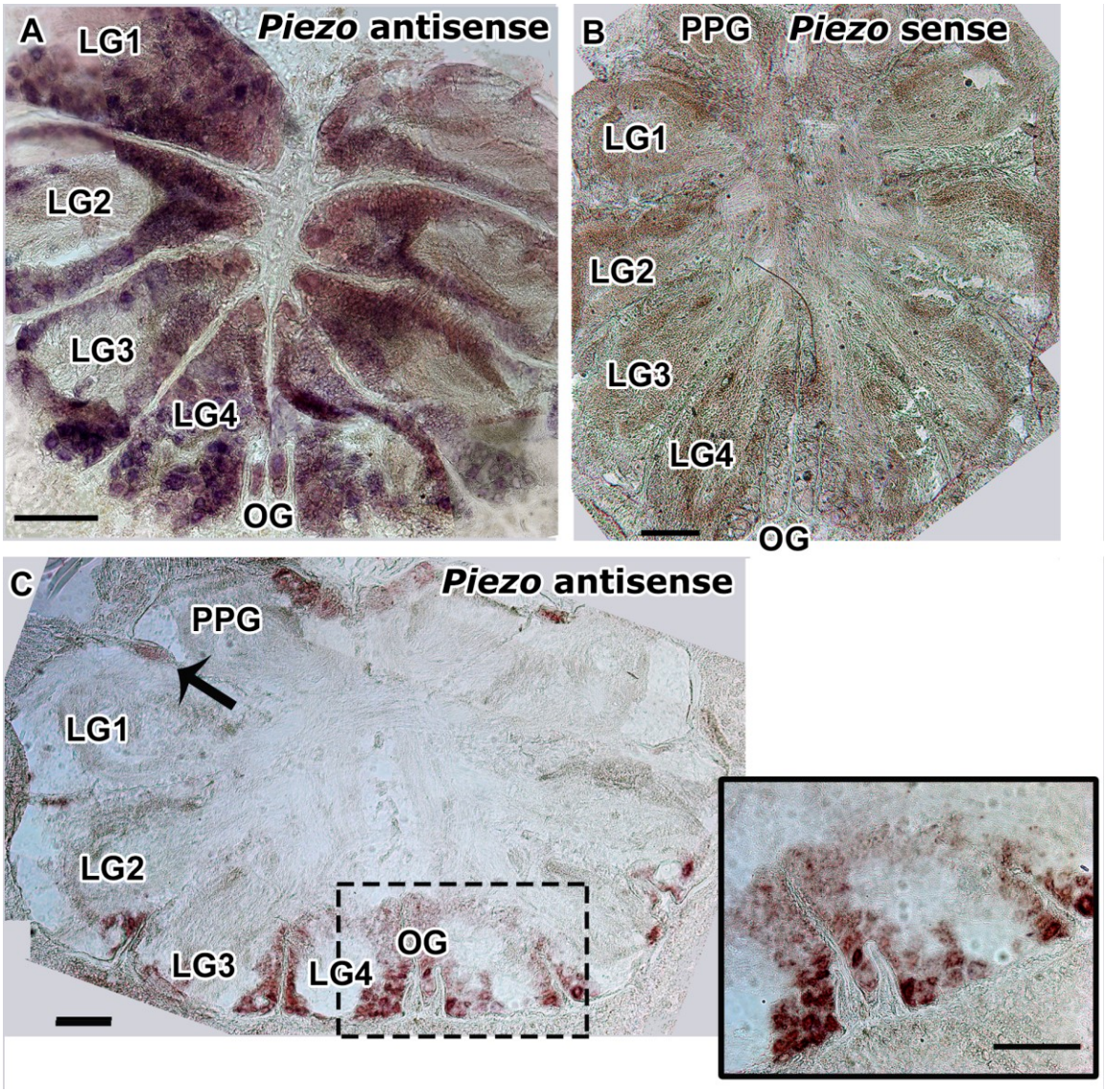

Figure 3.7. In-situ hybridization of subesophageal ganglion (Sub.eg) with *Piezo* probes. **(A)** Cross section of the ventral region of Sub.eg. shows strong signal for antisense probe in many cells that are located on the central and lateral areas of each leg ganglion (LG1-4) and opisthosomal ganglia (OG). **(B)** Cross section of the ventral region of Sub.eg. did not show any signal for the *Piezo* sense probe. **(C)** On the dorsal region of the Sub.eg. neuron cell bodies are located mainly on the lateral areas of each LG, OG and pedipalpal ganglia (PPG). At the anterolateral region of each leg ganglia there are distinct clusters of small neurons, and many of these neurons were also stained with the *Piezo* antisense probe (arrow). Inset shows the dashed region in C at higher magnification with distinctly labeled neurons of different sizes. Scale bars are 200 µm in all images.

In the subesophageal ganglion, the *Piezo* antisense probe produced very strong signal in the cell body region that is located in the ventral and lateral areas of each leg ganglia, opisthosomal and pedipalpal ganglia (Figure 3.7A). The sense probe did not produce any signal (Figure 3.7B). More sparsely labeled neurons were detected in the dorsal parts of the subesophageal ganglion (Figure 3.7C). In this area, the anterolateral neuron clusters were also labeled. The sizes of neurons that were labeled varied from 10 μm to 100 μm by diameter. Although each section had neurons that were clearly not labeled, it is not possible to make firm estimates about their percentage, since these sections were relatively thick (30-40 μm) and individual cells were often difficult to identify.

3.2.5. In-situ hybridization summary

The antisense probe for *Piezo* produced the clearest and most specific labeling in the VS-3 neurons and in many neurons of the Sub.eg. One of the antisense probes for ENaC channels, *Amil-1* also produced a signal, but this required a longer time to develop and the labeling was not only in the neurons but also in the surrounding glial and pigment cells. In addition, the probe for *Trp-1* (a *NompC* homologue) produced a signal in the VS-3 neurons, but this was restricted to the nuclear region and may indicate unspecific binding to DNA. Since the other probes tested here did not produce any specific labeling, even though the sequences were found in the hypodermis transcriptome (Figure 3.1), they are likely expressed in the leg muscle tissue that was removed from the patellar preparations.

3.3. Mechanotransduction channel inhibitors and an activator

Pharmacological approaches for identifying putative mechanotransduction channels are limited by the availability of specific inhibitors and activators of the various channel families. However, several investigators have used Ruthenium Red and GsMTx4 to block Piezo channels, so I tested their effects on the VS-3 neuron receptor current. The ENaC channel blocker amiloride has previously been shown to block the VS-3 neuron receptor current after a long incubation time (Höger et al. 1997). I also investigated amiloride effects on the excitability of these neurons. Yoda1 is a specific activator of some Piezo channels and I also tested how it affected the excitability of the VS-3 neurons.

These experiments were performed using continuous single-electrode current- and voltage-clamp with sharp intracellular electrodes. Typical responses of a slowly adapting Type B neuron to mechanical stimuli are shown in Figure 3.8. When the preparation was superfused in normal spider saline, the neuron fired one or more action potentials depending on the amplitude of the mechanical stimulus. Once the voltage-gated Na^+ channels were blocked with 1 μM TTX, the graded receptor current consisting of transient and sustained components could be recorded under voltage-clamp. The response of most mechanoreceptors to a similar ramp and-hold stimulus used here declines with time. This decline during sustained stimulus is not caused by decline in sensitivity but by the viscoelastic properties of the non-neural structures that transmit the stimulus (Barth 2019).

The average values for various parameters in all successful experiments under control conditions using mechanical and electrical stimulation are listed in Table 3.1

Table 3.1. Parameters for all successful experiments under control conditions.

	Membrane potential (mV)	Membrane resistance (MΩ)	AP threshold		AP amplitude (mV)		# of APs	
			µm	nA	M	E	M	E
Average	-68.5	61.2	0.4	0.7	37.2	40.5	3	4.9
SD	9.4	52	0.06	0.3	5	17.9	3.4	4.9
n	30	25	15	28	17	28	17	28

AP = action potential; SD = standard deviation; n = number of experiments; M = mechanical stimulation, E = electrical stimulation

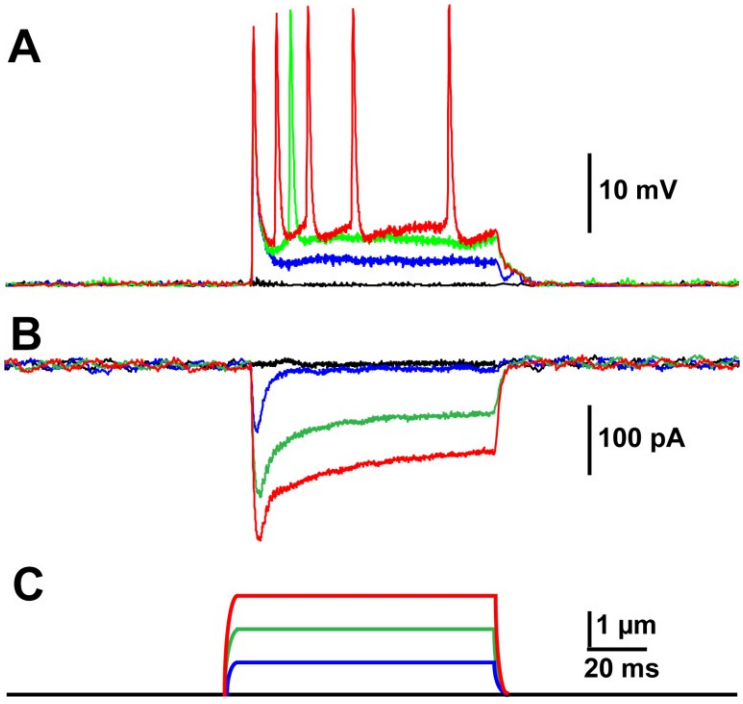

Figure 3.8. Typical responses of a Type B VS-3 neuron to mechanical stimulation. **(A)** shows the action potentials **(B)** shows receptor currents after 1 µM TTX was added to the superfusion solution **(C)** The mechanical stimuli.

3.3.1. Ruthenium Red had no effect on VS-3 neurons receptor current

Ruthenium Red (RR), an inorganic dye, has been shown to block many Ca^{2+} selective channels including the TRP channels, the mechanotransduction channel in the mammalian cochlear hair cells, and the mouse Piezo1 channel (Coste et al. 2012; Fettiplace and Kim 2014). I recorded the receptor currents from VS-3 neurons after the voltage-gated Na^{+} channels were blocked with 1 µM TTX. I then added 10 µM RR to the superfusion with the spider saline that was supplemented with TTX (=TTX-saline), and then recorded the receptor currents at 10 min intervals. A typical example of these experiments is shown in Figure 3.9A. In this experiment, the RR did not change the amplitudes of either the transient or the sustained components of the receptor current. After a long wash in TTX-saline without RR, the receptor current remained similar to the control. The average receptor current amplitudes from eight neurons after 20 min incubation in RR + TTX-saline are shown in the bar graph of Figure 3.9B. There were no statistically significant differences between the amplitudes of peak receptor currents when tested with a paired t-test ($p = 0.43$, $t = 0.19$, $df = 7$).

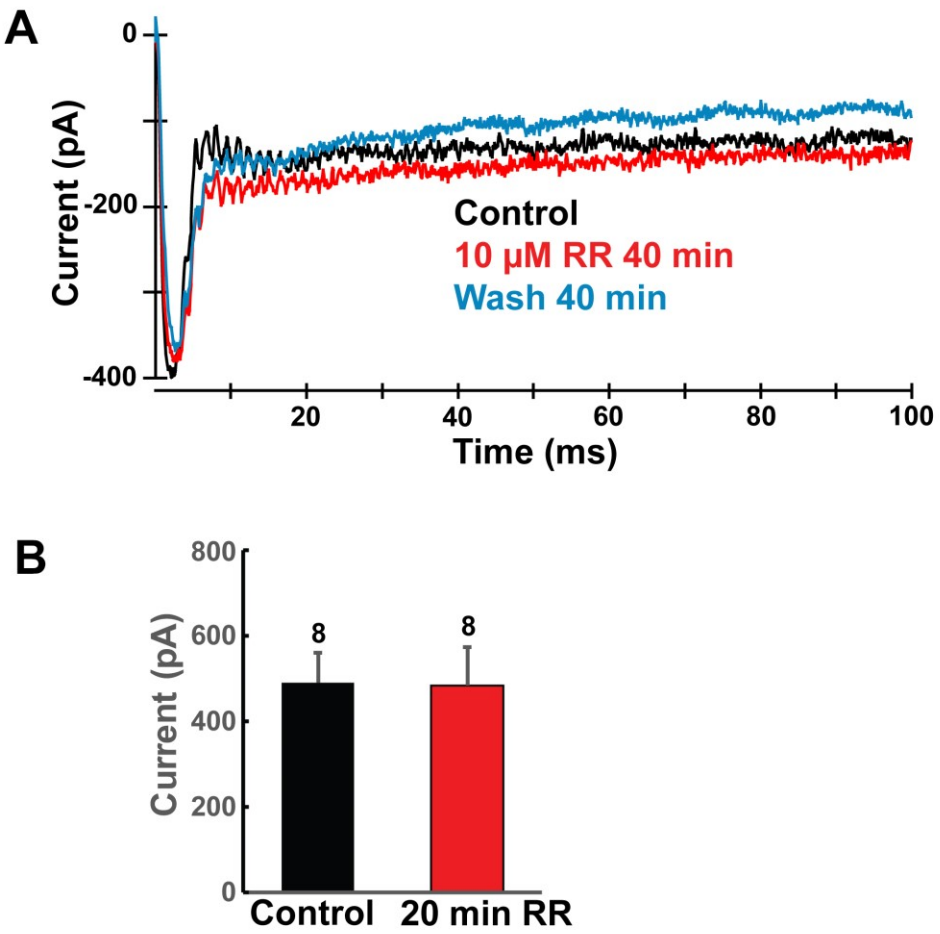

Figure 3.9. Ruthenium Red had no effect on VS-3 neuron receptor current. **(A)** The receptor currents with 3-µm stimulus under control conditions (TTX-saline), 40 min in RR + TTX saline and after 40 min wash in TTX-saline. **(B)** Bar graph shows the average (±SE) peak receptor currents in eight neurons under control conditions and after 20 min in RR. Numbers of experiments are indicated above each bar.

In this series of experiments, most cells died after about 30 min in RR. However, two experiments where the neurons were alive for an hour did not show any change in the receptor current amplitudes. Other neurons either died earlier or in some cases had smaller receptor current after 30 min, but there was no recovery after even very long washes. Since RR is a rapidly acting drug (Malécot et al. 1998) and I used high

concentration, there should have been at least some change within 20 min in most neurons to conclude that RR is an inhibitor of the VS-3 mechanotransduction channels.

3.3.2. GsMTx4 had no effect on VS-3 neuron receptor current

GsMtx4 peptide was isolated initially from the venom of the tarantula *Grammastola spatulata* and shown to selectively inhibit several types of stretch activated ion channels, including the mammalian Piezo1 and Piezo2 channels (Suchyna 2017) and the mechanotransduction channel in cochlear hair cells (Fettiplace and Kim 2014). I used a synthetic D-amino acid form analog of GsMTx4, at 5 μM concentration to test if it inhibits VS-3 neuron receptor current. Figure 3.10A shows typical recordings of receptor currents under control conditions (TTX-saline), 30 min and 60 min after GsMTx4 was added to the superfusion. The receptor current amplitude in this experiment was slightly larger after 60 min in GsMTx4 than under control conditions. When the average peak receptor currents from several experiments were compared (Figure 3.10B) using paired t-tests, there were no statistically significant differences after 30 min ($p = 0.11$, $t = 1.48$, $df = 4$) or 50 min ($p = 0.12$, $t = 1.35$, $df = 4$).

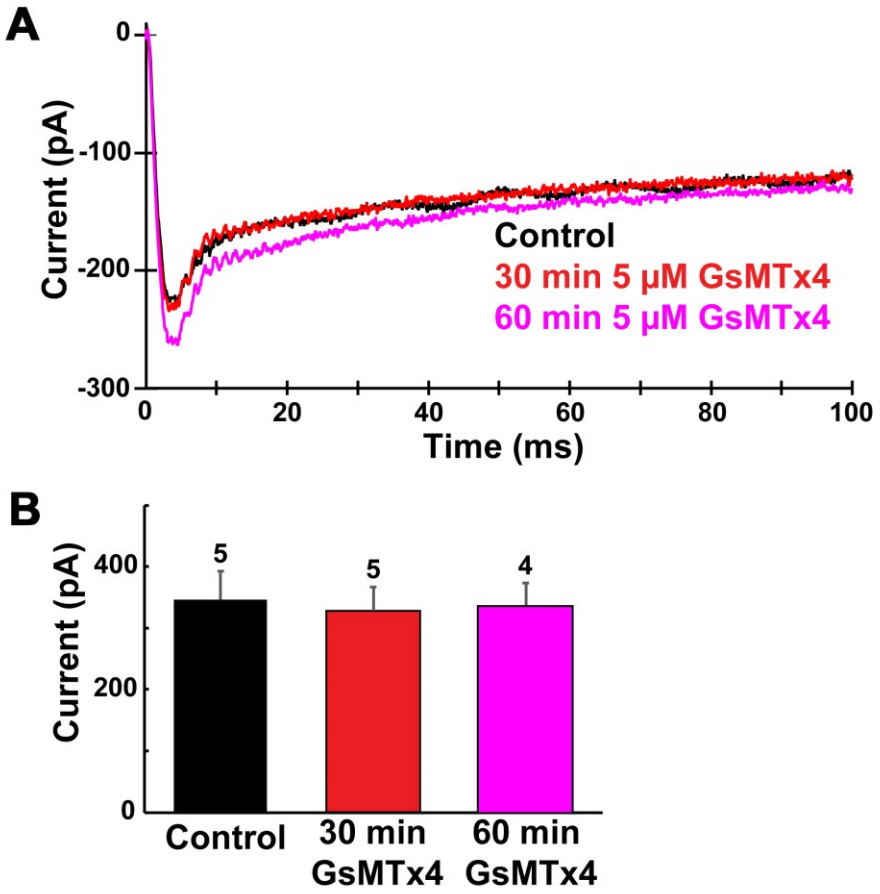

Figure 3.10. GsMTx4 had no effect on VS-3 neuron receptor current. **(A)** Receptor currents of a VS-3 neuron in response to 3 µm mechanical stimulus under control conditions (TTX-saline) and 30- and 60-min incubation in 5 µM GsMTx4 in TTX-saline. **(B)** Bar graphs show average (±SE) peak receptor currents under control conditions, and after 30 and 60 min in GsMTx4. Numbers of experiments are indicated above each bar.

3.3.3. Yoda1 had an excitatory effect on VS-3 neurons

Yoda1 is an agonist of mammalian Piezo1 ion channels (Syeda et al. 2015). The Piezo channels were found in the dendrites and axons of the VS-3 neurons (Figure 1.6) suggesting that their activation could have effects that are not limited to modulation of receptor current. Therefore, I tested Yoda1 under current-clamp on neurons that were superfused in normal saline and able to fire action potentials.

When 25 µM Yoda1 was applied to the superfusion solution, four out of ten VS-3 neurons fired action potentials without electrical or mechanical stimulation (Figure 3.11). This firing became more pronounced when the drug was applied multiple times. The resting membrane potential did not change when Yoda1 was in superfusion solution.

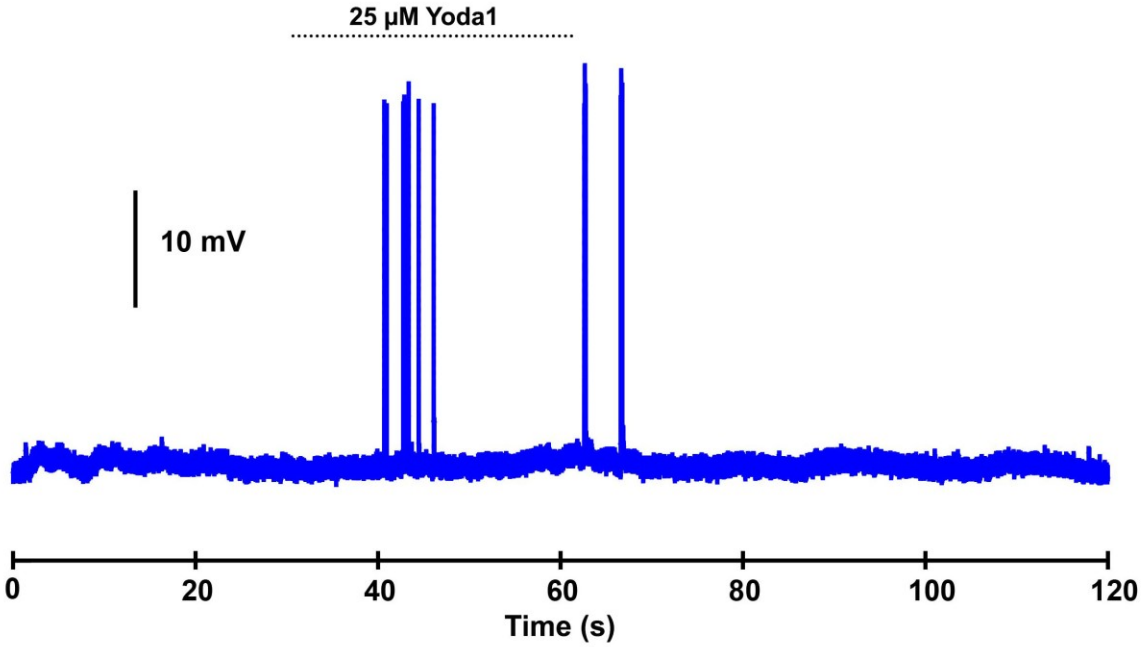

Figure 3.11. Effect of Yoda1 application on a VS-3 neuron. During and immediately after application of 25 µM Yoda1 this neuron fired brief bursts of action potentials.

The longer-term effect of Yoda1 on VS-3 neuron receptor potential and excitability is shown in Figure 3.12. When the neurons are stimulated mechanically under current-clamp, they produce a receptor potential and, when the threshold is reached, they fire action potentials on top of the receptor potential. After the neurons were superfused in saline supplemented with 25 µM Yoda1 for 10-30 minutes, the receptor potential was larger and in some cases the cells fired more and somewhat larger action potentials. The effect on receptor potential amplitude was statistically significant (paired t-test: $p = 0.04$, $t = -2.05$, $df = 7$).

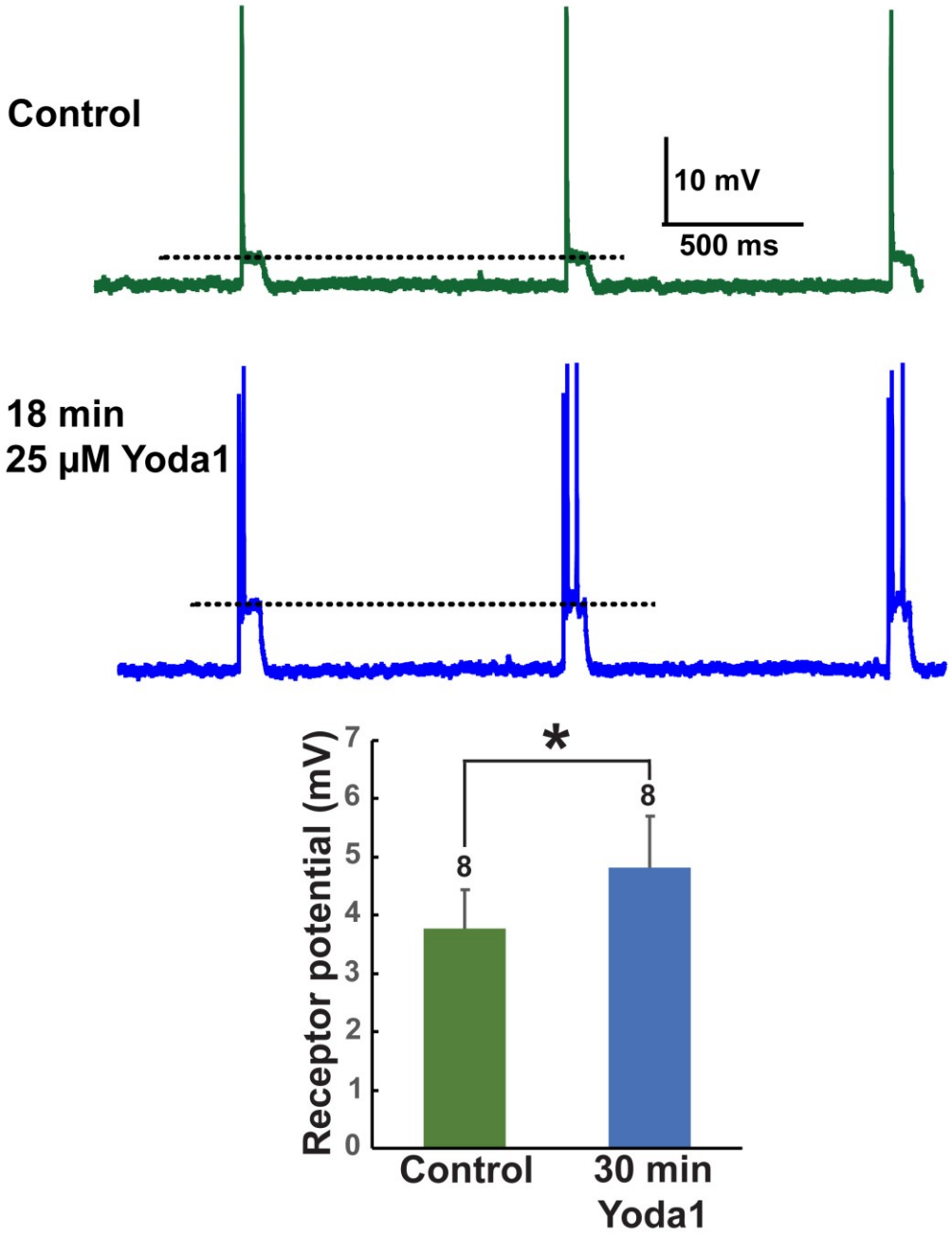

Figure 3.12. Yoda1 effects on VS-3 neuron receptor potentials and excitability. The green and blue traces show a continuous recording of voltage responses to mechanical stimulus when the preparation was superfused in normal saline (green) and 18 min after 25 µM Yoda1 was added to the superfusion (blue). Dashed lines indicate the receptor potentials. Bar graphs show the average receptor current of eight neurons (±SE) in normal saline (green) and 30 min in saline supplemented with Yoda1 (blue).

Figure 3.13 shows the Yoda1 effects on the numbers of action potentials and their amplitudes when the VS-3 neurons were stimulated either mechanically or electrically. The neurons fired larger action potentials after 30 min in Yoda in response to mechanical stimulus (Figure 3.13A, paired t-test: p = 0.007, t = -3.42, df = 6) but there was no statistically significant difference in AP amplitudes when the cells were stimulated electrically (Figure 3.13B, paired t-test: p = 0.0618, t = -1.79, df = 6). The number of action potentials in response to mechanical stimulus did not change significantly after Yoda1 incubation (Figure 3.13C). However, the mechanical stimulator was adjusted to produce only one action potential at the beginning of most experiments and this data was not normally distributed making it difficult to test reliably and especially prevented testing whether the actual threshold for firing action potentials changed. The number of action potentials in electrically stimulated neurons increased significantly after Yoda1 treatment (paired t-test: p = 0.00997, t = -3, df = 7). In summary, Yoda1 had excitatory effects on both mechanically and electrically stimulated VS-3 neurons.

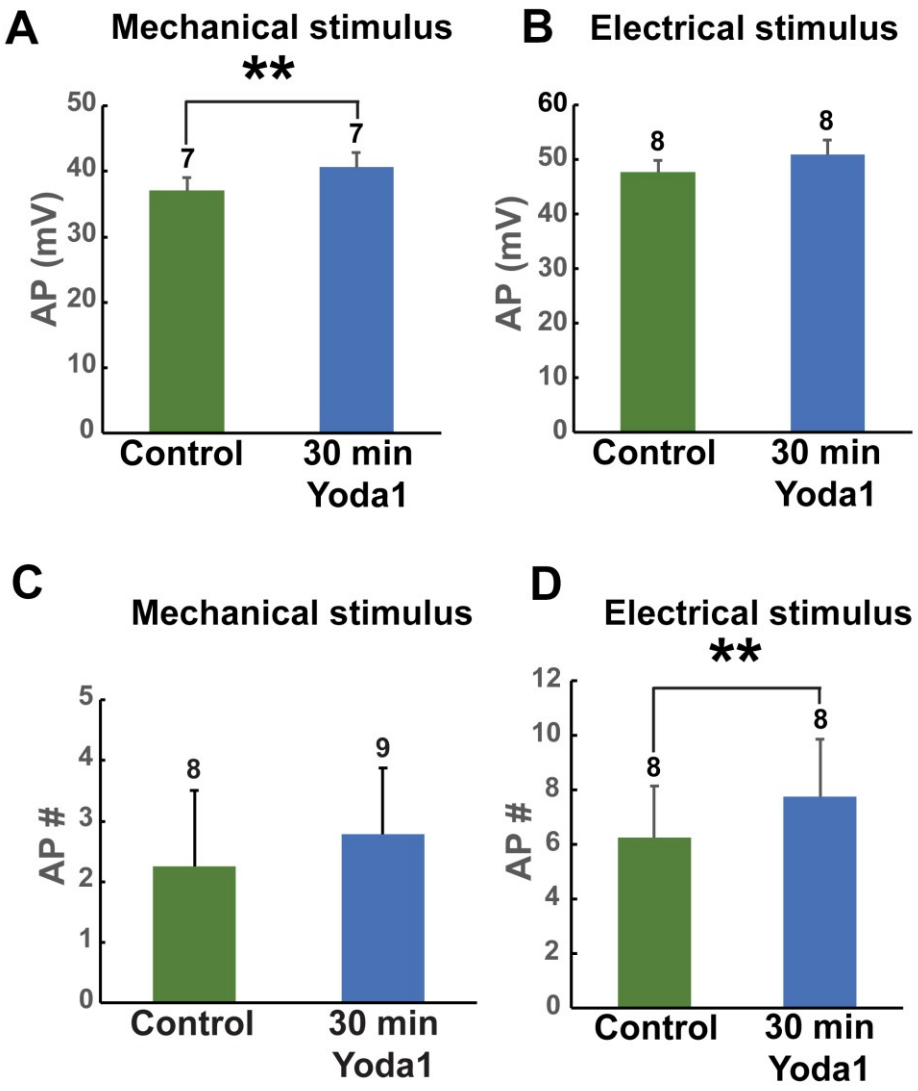

Figure 3.13 Yoda1 effects on VS-3 neuron action potentials. The action potential (AP) amplitudes in response to 1.5 µm mechanical stimulus **(A)** and 1.5 nA electrical stimulus **(B)** under control conditions and after 30 min in superfusion with 25 µM Yoda1. The number of action potentials with the same stimuli in mechanically stimulated neurons **(C)** and in electrically stimulated neurons in **(D)**.

3.3.4. Amiloride effects on VS-3 neuron excitability

Amiloride is a blocker of epithelial sodium channels (ENaC) (Canessa et al. 1994) and it has been shown to block the *C. elegans* MEC-4 channel that is a member of ENaC

family (O'Hagan et al. 2005). Interestingly, it has also been discovered that the *Drosophila* Piezo protein is sensitive to amiloride (Suslak et al. 2015). The *C. salei* VS-3 neuron mechanotransduction current was almost completely blocked by 1 mM amiloride after about one-hour incubation period (Höger et al. 1997) but its effects on the neuron's excitability have not been investigated. If the VS-3 neuron receptor current flows through amiloride sensitive ion channels, amiloride should inhibit mechanically induced action potentials without any effects on electrically induced action potentials. To test if this hypothesis is true, I performed a series of experiments to determine the effects of 1 mM amiloride on the VS-3 neurons responses to mechanical and electrical stimuli.

When the neurons were stimulated with a mechanical step stimulus while they were superfused in normal spider saline, they fired one or more action potentials depending on the type of the neuron and the strength of the stimulus. The receptor potential could also be measured in these experiments as shown in Figure 3.14. When 1 mM amiloride was added to the superfusion, the neurons were still firing action potentials, but the receptor potential was either smaller or completely abolished as seen in the experiment in Figure 3.14. After 30 min incubation in saline supplemented with 1 mM amiloride the change in receptor potential amplitude was statistically significant (paired t-test: $p = 0.0415$, $t = 1.98$, $df = 8$). There were no further changes in receptor potential amplitudes after longer term exposure to amiloride.

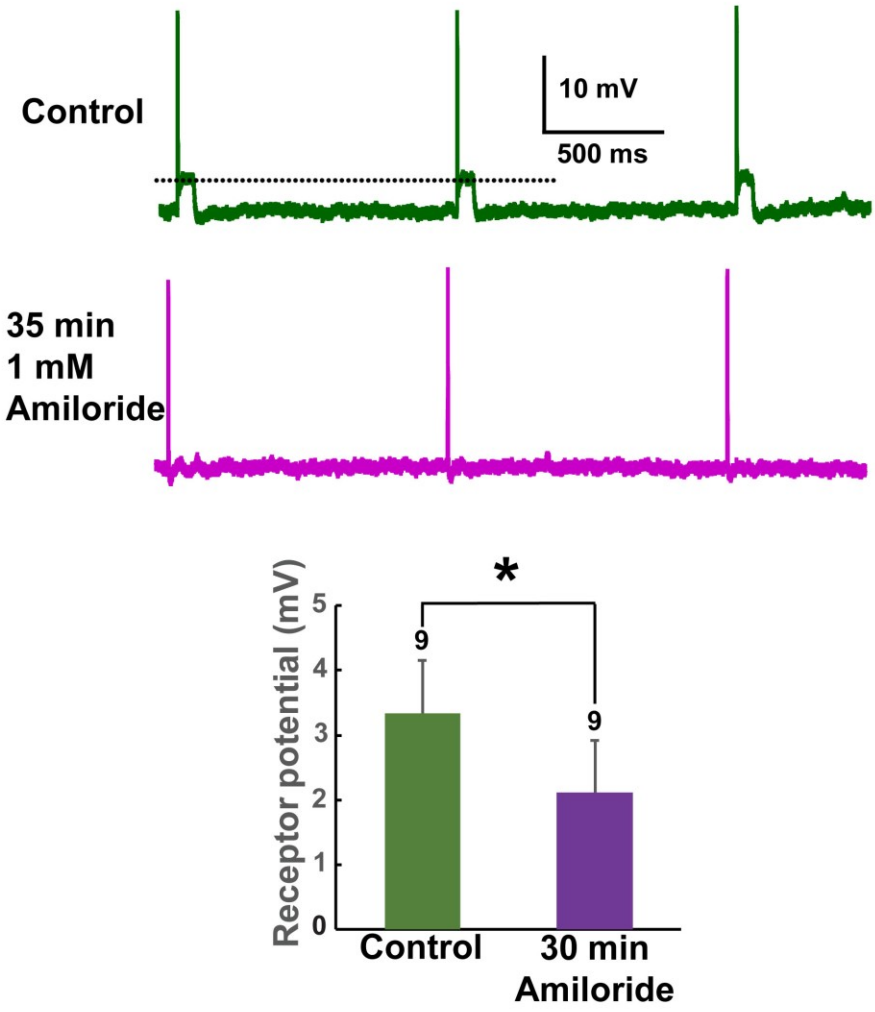

Figure 3.14. Amiloride effect of VS-3 neurons receptor potential. A series of voltage responses to mechanical step stimuli under control conditions and 35 min after superfusion in spider saline supplemented with 1 mM amiloride. In both cases the neuron fired one action potential in response to similar stimulus, but the receptor potential was not detectable after amiloride. The dotted line indicates how the receptor potential was measured. Bar graph shows the average receptor potential amplitudes (± SE) under control conditions and after the neurons were superfused 30 min in saline with 1 mM amiloride. Numbers of experiments are indicated above each bar.

Amiloride effects on VS-3 neurons were further investigated using different sizes of mechanical and electrical step stimuli (Figures 3.15 and 3.16). With both types of stimuli, the number of action potentials was lower 30 min after the start of amiloride

superfusion and slowly decreased further. (One-way Anova for mechanically stimulated neurons: $p = 0.0328$, $F = 4.26$ [2,16], Figure 3.15B. For electrically stimulated neurons: $p = 0.017863$, F=5.44 [2,14], Figure 3.16B). The amplitude of individual action potentials also became smaller when neurons were stimulated mechanically ($p = 0.0403$, F =3.95 [2,16] Figure 3.15C). For electrically stimulated neurons, the size of action potentials was difficult to estimate, since the membrane resistance also increased significantly ($p = 0.00641$, $F = 7.4$ [25,14]) as can be seen in Figure 3.16A and C.

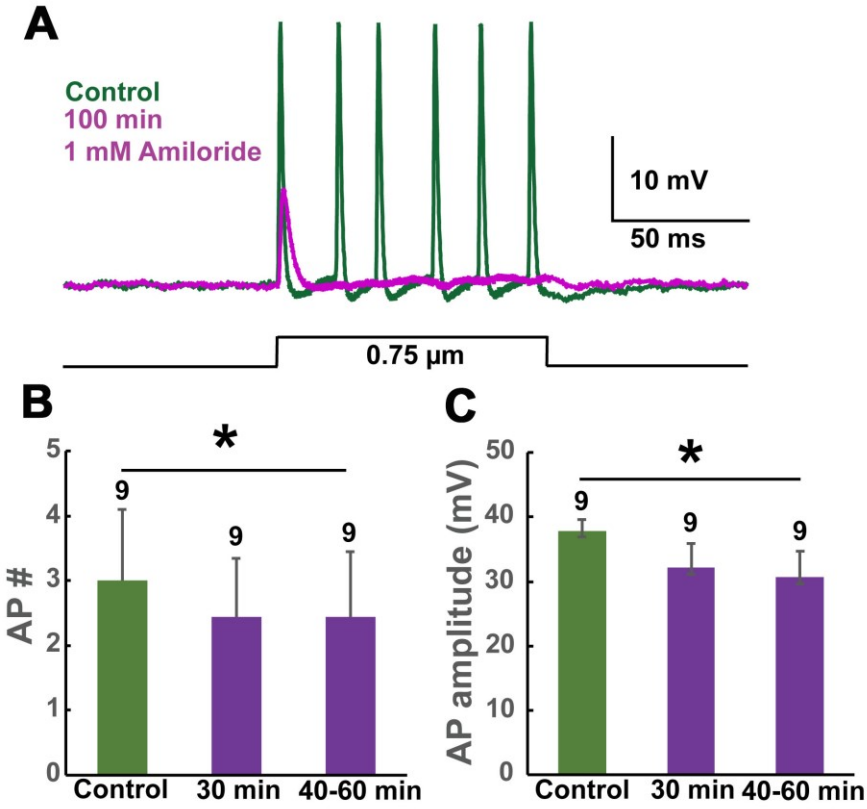

Figure 3.15. Amiloride effects on mechanically stimulated VS-3 neurons. **(A)** The voltage response of a Type B neuron under control conditions (normal spider saline; green) and after 100 min superfusion in saline supplemented with 1 mM amiloride (purple). The mechanical stimulus is shown below. Bar graphs showing the average number **(B)** and amplitude **(C)** of mechanically induced action potentials (±SE) under control conditions and after superfusion in amiloride supplemented saline for 30 and 40-60 min. Numbers of experiments are indicated above each bar.

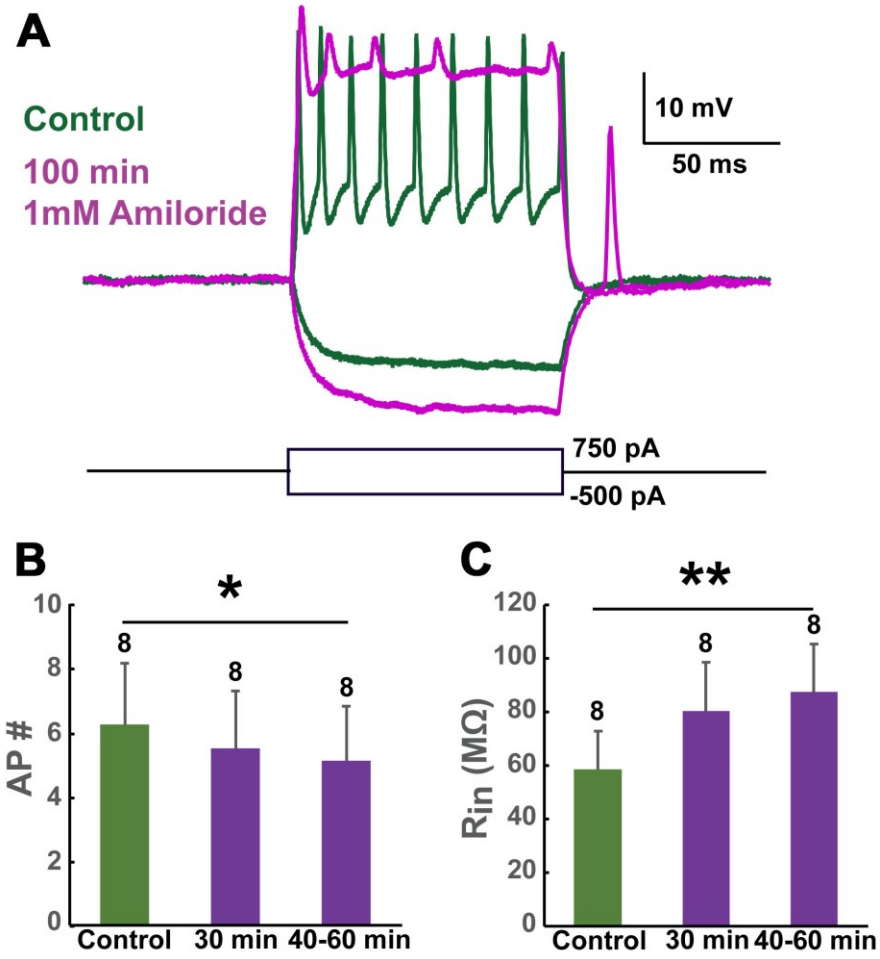

Figure 3.16. Amiloride effects on electrically induced action potentials and membrane resistance. **(A)** The voltage response of Type B VS-3 neuron to electrical step stimuli under control conditions and after 100 min superfusion in saline supplemented with 1 mM amiloride. The sizes of positive and negative stimuli are shown below. Bar graphs show the numbers of action potentials **(B)** and the magnitude of membrane resistance (±SE) **(C)** under control conditions and after superfusion in saline supplemented with amiloride for 30 and 40-60 min. Numbers of experiments are indicated above each bar. The membrane resistance was estimated at the end of a -500 pA stimulus by Ohms law.

In conclusion, amiloride reduced the receptor potential amplitude and reduced the excitability in both mechanically and electrically stimulated neurons but did not completely block the action potential firing even after a long-term incubation. Amiloride

increased membrane resistance indicating that a conductance was blocked, and this may have caused the inhibitory effects.

3.4. Knockdown of *C. salei Piezo* by RNA interference

The final part of my thesis work involved the initial development of an experimental approach using RNA interference (RNAi) to knockdown potential mechanotransduction genes in *C. salei*. This method has been successfully used in this laboratory and many others to investigate roles of various genes in insects by injecting the dsRNA into their head or body (e.g., French et al. 2015; Hennenfent et al. 2019) Since the spiders are large and have high hemolymph pressure it would be very difficult to inject an adequate amount of dsRNA into their body. Feeding dsRNA is also not feasible, since spiders only eat live prey. Therefore, we used a method where patellar cuticular preparations were maintained in culture media supplemented with dsRNA for up to three days. Control preparations were dissected and treated the same way but had no dsRNA in the culture media.

The aim was to knock down the *Piezo* gene, and to record potential changes in VS-3 neuron responses to electrical and mechanical stimulation. Establishing this method has been very challenging. Problems with contamination and fragility of the tissue have made it difficult to get consistent results. However, my results are very promising although number of successful electrophysiological experiments was low and therefore these results are preliminary. Figure 3.17 shows experiments from two preparations that were kept three days in culture. The neurons in control preparation had normal responses to both electrical and mechanical step stimuli while the cells in the preparation that was maintained three days in culture media with *Piezo* dsRNA had normal responses to

electrical stimulus but did not respond mechanical stimulus. It is notable that the latter cell was a Type B neuron that would normally have a low threshold for both types of stimuli. I have recorded similar results from two control neurons and five neurons that were treated with dsRNA. I also performed similar experiments on preparations that were maintained only one day in culture, and in this case three dsRNA treated neurons had no response to mechanical stimulus, while one fired an action potential but had high threshold. However, the two control preparations in this run died very quickly before I obtained results from mechanical stimulation.

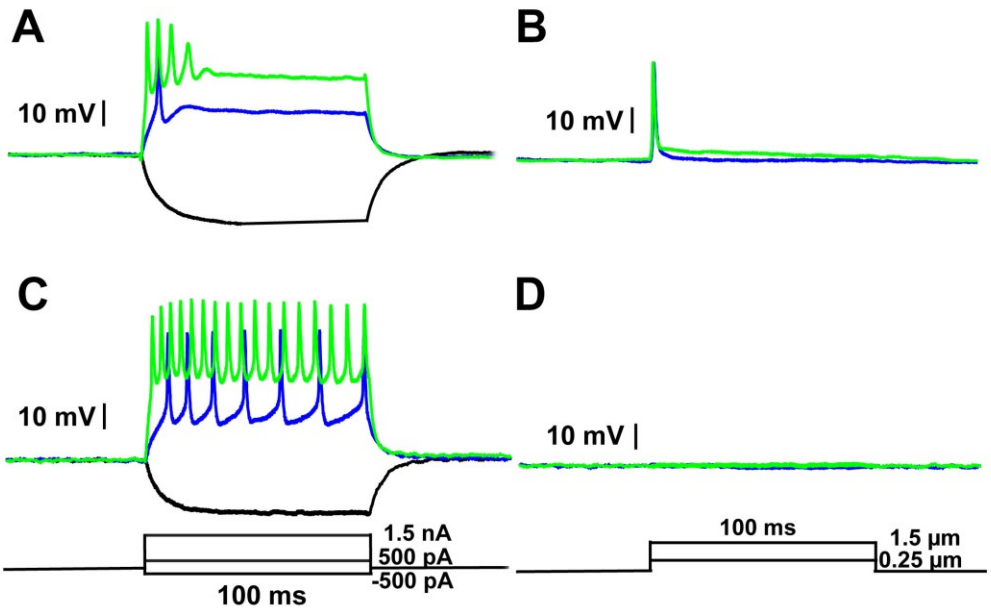

Figure 3.17. Effects of *Piezo* knockdown on electrical and mechanical action potentials. Type A neuron from a control VS-3 organ that was maintained in tissue culture for 3 days had normal responses to electrical **(A)** and mechanical **(B)** stimuli. Type B neuron that was maintained 3 days in culture media supplemented with dsRNA for *Piezo* had normal responses to electrical stimuli **(C)** but it did not respond to mechanical stimuli **(D)**.

CHAPTER 4. DISCUSSION

My thesis work intended to discover the identity of the mechanotransduction channel in the *C. salei* VS-3 neurons. I used in-situ hybridization to determine putative mechanotransduction channel genes that are expressed in VS-3 neurons, pharmacological tools to test whether known inhibitors and an activator modulate the mechanotransduction current or excitability of these neurons, and I participated in the development of a method to knock down genes that code putative mechanotransduction channels. My results support the theory that Piezo protein, either alone or together with an amiloride sensitive ion channel, is the mechanotransduction channel in VS-3 neurons. The evidence for this conclusion is discussed below.

4.1. Expression of putative mechanotransduction channels in *C. salei*

From the nine probes that were tested using in-situ hybridization, only the *Piezo* antisense probe produced strong specific labeling in VS-3 neurons and other sensory neurons of the hypodermis. This probe also labeled many neurons in the subesophageal ganglia. When I tested the *C. salei* Piezo antibody on the patellar hypodermis in my Honor's thesis, it strongly labeled the dendrites and axons of all sensory neurons as well as the leg nerves. This antibody was also tested on sections of the spider CNS (Torkkeli et al. 2018) and it labeled cell bodies in the same areas of subesophageal ganglia as I found using in-situ hybridization. In addition to the cell bodies, antibody labeling was also strong in many nerve fibers that project to the legs, pedipalpal and opisthosomal ganglia. Widespread expression of Piezo proteins is common in both vertebrate and invertebrate tissues and implies that they have multiple functions, such as in cell volume regulation and cell migration. For example, in larval and adult *Drosophila*, Piezo protein

was found in all parts of many sensory and other neurons and it was also present in non-neural tissue (Kim et al. 2012). The vertebrate Piezo2 protein is mostly found in neurons while the Piezo1 is expressed in a variety of non-neural tissue including blood vessels, red blood cells, epithelial cells of the bladder and kidneys (Murthy et al. 2017). The *C. salei* Piezo protein is only expressed in sensory neurons and a variety of subesophageal neurons that, based on their size and location, include motor neurons (Babu and Barth 1984). Piezo expression in *C. salei* and other animals is so widespread that it must have a variety of important functions that remain to be discovered.

The *Amil-1* antisense probe labeled the VS-3 neurons after overnight dye reaction. *Amil-1* labeling was also seen in glial and pigment cells and overall in the hypodermis. Therefore, it is possible that this labeling was not specific and these results should be confirmed with a different probe against the same gene. Amiloride sensitive epithelial sodium channels are widely expressed in many different types of tissues (Simon et al. 2010; Kashlan and Kleyman 2011). So, it would not be surprising to find these channels in other cells than neurons. DEG/ENaC channels MEC-4 and MEC-10 have been implicated in mechanotransduction and found to be expressed in *C. elegans* neurons that detect gentle touch (O`Hagen et al. 2005; Cueva et al 2007). In *Drosophila*, the ENaC channel *pickpocket* (*ppk*) and the *Piezo* channel are expressed in sensory neurons that mediate nociception, while deletion of either channel removed mechanical nociception suggesting that these two channels function in parallel pathways to detect mechanical pain (Kim et al. 2012).

The *Trp-1* antisense probe labeled the nuclear area of VS-3 neurons. This may be unspecific labeling, where the probe binds to the DNA, but it is also possible that this

labeling is in the endoplasmic reticulum that surrounds the nucleus. This probe should be tested on sections to determine the exact location of the labeling. The *C. salei Trp-1* gene is homologous to the *Drosophila NompC* that, along with TRP-channels Nanchung-Inactive, has been associated with insect mechanotransduction (Walker et al; 2000; Cheng et al. 2010; Lee et al. 2010; Effertz et al. 2011). The mechanotransduction channels in insects are located in a K^+ rich receptor lymph space with a high transepithelial potential while the spider organs lack the transepithelial potential and are surrounded by extracellular solution with high Na^+ concentration (Grünert and Gnatzy 1987). So far, the *C. salei* transcriptome searches have not found homologues for *nanchung* or *inactive*, suggesting that either their abundances are very low, or they are not expressed at all. It is likely that TRP channels are not as important in *C. salei* mechanotransduction as they are in insects.

Interestingly, the relative abundances of all three transcripts that produced some labeling in VS-3 neurons was higher in the hypodermis than in the CNS (Figure 3.1), suggesting that they are more important in the peripheral than central locations. Six other probes did not produce specific labeling in the VS-3 neurons or any other cells of the patellar hypodermis. Since all these transcripts were found in the hypodermis, in some cases with very high relative abundances, they are most likely expressed in the leg muscle, some of which was included into the tissue used for creating the transcriptomes (French 2012).

4.2. Mechanotransduction channel pharmacology

Ruthenium Red (RR) and GsMTx4 had no effects on VS-3 neuron receptor current. RR is a nonspecific inhibitor of many cation sensitive channels including several

types of TRP channels. It blocks the receptor current in mammalian cochlear hair cells, which is believed to flow via TMC channels, and it also blocked the mechanically activated inward currents of heterologously expressed mouse Piezo1 and Piezo2 channels (Malecot et al. 1998; Coste et al. 2010; Pan et al. 2018). However, RR did not inhibit *Drosophila* Piezo channels that were expressed in HEK293T cells (Coste et al. 2012). When a C-terminal half of *Drosophila* Piezo sequence was replaced with mouse Piezo, the resulting chimeric channel was sensitive to RR indicating that the binding site for RR is in the C-terminus, and that it is different in these two channels (Coste et al. 2015). If Piezo is the *C. salei* mechanotransduction channel, the lack of effect by RR suggests that, like *Drosophila*, it does not have the binding region for RR.

The tarantula toxin GsMTx4 has been shown to inhibit many cation selective stretch activated channels including some TRP channels, the mammalian Piezo1 and Piezo2 and the mechanotransduction channel in the cochlear hair cells (Fettiplace and Kim 2014; Alcaino et al. 2017; Suchyna 2017). GsMTx4 does not seem to block the pore of mechanotransduction channels, but rather inserts itself into the membrane in a tension-dependent manner and compromises the distribution of tension near the channel (Gnanasambandam et al. 2017). This may be the reason why inhibition observed on the mouse Piezo1 channel could be overcome by increasing pressure on the channel (Bae et al. 2011) and it is possible that the blocking effect on VS-3 neurons was overcome by the mechanical stimulator. Most of the previous work on GsMTx4 effects on Piezo channels has involved single-channel or whole-cell patch clamp on cultured cells. These are very different to sharp electrode intracellular recordings on intact tissue where the VS-3 neurons are heavily enwrapped by glial cells. It is possible that this large molecule did

not reach the dendritic region even after a very long incubation time and high concentration of GsMTx4, or alternatively the blocking effect is very transient.

Yoda1 has been shown to increase the sensitivity and slow the inactivation phase of mechanically activated currents in cultured cells that express mouse Piezo1 with no effect on cells that express the Piezo2 channels (Syeda et al. 2015). Lacroix et al. (2018) have determined the motif that recognizes Yoda1 on mouse Piezo1 and within this region 21 residues are not conserved between mouse Piezo1 and mouse Piezo2. However, the exact residues that recognize Yoida1 have not been identified. To my knowledge Yoda1 has not been tested on *Drosophila* or any other invertebrate Piezo channels, but my results suggest that Yoda1 activates *C. salei* Piezo protein. Yoda1 stabilizes the open state of Piezo1 channels and it can activate the channel without mechanical stimuli (Syeda et al. 2015). The latter finding could explains why Yoda1 application without any mechanical stimulus, induced action potentials in many of my experiments. When the VS-3 neurons were superfused for longer times (10-30 min) in saline supplemented by Yoda1, it had an overall excitatory effect on the VS-3 neurons. The amplitudes of both the mechanically induced receptor potentials and action potentials were larger, and the neurons also fired more action potentials with mechanical stimuli, although the latter effect was not statistically significant. These findings suggest that the mechanotransduction current in VS-3 neurons is sensitive to Yoda1. However, this result needs to be confirmed with voltage-clamp experiments of the receptor current itself.

Yoda1 had a very clear excitatory effect on action potential firing when the VS-3 neurons were stimulated with an electrical step stimulus. If Yoda1 indeed activates *C.*

salei Piezo channels, this finding is consistent with my immunocytochemical finding that these channels are expressed in both the dendrites and axons.

Amiloride, the known blocker of epithelial sodium channels, has previously been shown to reduce the receptor current in the VS-3 neurons after a long incubation period (Höger et al. 1997). For this study, I investigated the amiloride effects on the excitability of the VS-3 neurons. If an amiloride sensitive ENaC channel alone is responsible for the receptor current, these neurons could not fire action potentials in response to mechanical stimulus while the electrically induced firing would not be affected. I observed a reduction in receptor potential amplitude, but even after long period of amiloride in the bath, the mechanically stimulated VS-3 neurons still fired action potentials. The amplitude and number of action potentials declined slowly in both mechanically and electrically stimulated neurons although the actual amplitude of electrically stimulated action potentials was difficult to measure, since the membrane resistance also increased.

These results demonstrate that amiloride has a more wide-ranging effect on VS-3 neurons than inhibition of the receptor current. Increase in membrane resistance indicates that an ion conductance is blocked, and this makes it more difficult for the neurons to fire action potentials what ever kind of stimulus is used. This change in conductance may also have caused the reduction of receptor potential and receptor current. The *Amil-1* in-situ hybridization results suggest that at least one type of ENaC channel is expressed in VS-3 neurons and other cells in the organ. It is possible that this channel is responsible for amiloride effects and it may regulate epithelial transport that indirectly reduced excitability.

These results do not exclude the possibility that an amiloride sensitive channel is involved in VS-3 neuron mechanotransduction. One possibility is that Amil-1 and Piezo channels are both involved in mechanotransduction as has been suggested for the *Drosophila ppk* and Piezo channels in larval multidendritic neurons (Kim et al. 2012).

4.3. Knockdown of *Piezo* gene

Since the pharmacology of putative mechanotransduction channels is limited to generic inhibitors of ion channels and an activator of one type of vertebrate Piezo channel, it is difficult to draw firm conclusions on the identity of the mechanotransduction channel based on the results shown in this thesis. A significantly better approach is to specifically silence a gene of interest. To better understand the role of Piezo protein in VS-3 neurons, I participated into the development of a method to knock down *Piezo* gene using RNAi. Since we had to develop a tissue culture system for preparations that are very difficult to dissect using sterile techniques, we encountered severe problems with contamination and survival of the cells. Despite these issues, I performed some successful electrophysiology experiments. In these experiments, the control neurons responded to electrical and mechanical stimulation as expected, while *Piezo* knockdown neurons responded only to electrical stimulation and failed to respond to mechanical stimulation. However, the number of experiments was low and actual knockdown of *Piezo* gene needs to be confirmed by RT-qPCR. This method is also challenging due to the small amount of tissue available for each experiment. However, the electrophysiological experiments that I performed provide valuable preliminary results for discovering the functions of the Piezo protein and show that experiments can

be done using this method. In fact, it was relatively easier to impale the neurons that had been in culture when compared to fresh preparations.

4.4. Conclusions

Despite the limitations that were mentioned throughout this thesis, my study supports the view that the mechanotransduction channel in the *C. salei* VS-3 neurons could be the Piezo protein and it may function together with an amiloride sensitive channel. The evidence provided here and earlier in my Honor's thesis fulfill the first criterion for the Piezo protein to be considered a mechanotransduction channel in a mechanosensory cell (Katta et al. 2015): "*The channel must be expressed in the sensory cell responsible for mechanotransduction and localized in the correct position within the cell."* In-situ hybridization with an antisense probe for *Piezo* produced strong, specific signal in the VS-3 neurons. In my Honor's thesis I used a custom-made antibody for *C. salei* Piezo protein, and it labeled the VS-3 neuron dendrites. I also provide preliminary evidence for the second criterion: "*The channel must be necessary for generating an electrical response to the mechanical stimuli."* Knockdown of *Piezo* gene by RNA interference removed responses to mechanical stimuli. However, this needs to be confirmed with larger numbers of experiments. The *Amil-1* gene is also likely expressed in the VS-3 neurons, and it may participate in mechanotransduction. I also found that the *Piezo* gene is expressed widely in neurons of the spider subesophageal ganglion and probably has multiple roles in these neurons. The pharmacological part of my work was limited by the availability of specific agonists and antagonists for different channel families. However, increase in excitability by Yoda1 also supports the role of Piezo as the mechanotransduction channel while the effects of both Yoda1 and amiloride indicate that

they may act on other channels in addition or instead of those directly involved in mechanotransduction.

4.5. Future directions

My studies have yielded exciting revelations for the putative mechanotransduction channels, especially the Piezo protein, in *C. salei* VS-3 neurons. The RNAi experiments should be continued and include RT-qPCR to confirm the *Piezo* knockdown. Furthermore, different conditions for in-situ hybridization and probably new probes should be tested for *Amil-1* and *Trp-1* to confirm the results. If successful, custom-made antibodies should be created and tested in immunocytochemistry and Western blot analysis to determine their localizations in VS-3 neurons. Knockdown of any putative mechanotransduction channel using RNAi followed by electrophysiology should also be performed. I only tested two of the four criteria that define a mechanotransduction channels for the Piezo protein. For the third and fourth criteria, the *Piezo* gene should be expressed in a heterologous system to test whether it forms mechanosensitive ion channels, and this would also allow investigation into additional properties of these channels such as ionic selectivity.

References

Adams CM, Anderson MG, Motto DG, Price MP, Johnson WA, Welsh MJ (1998) Ripped pocket and pickpocket, novel *Drosophila* DEG/ENaC subunits expressed in early development and in mechanosensory neurons. J Cell Biol 140:143-152.

Alcaino C, Knutson K, Gottlieb PA, Farrugia G, Beyder A (2017) Mechanosensitive ion channel Piezo2 is inhibited by D-GsMTx4. Channels (Austin) 11:245-253.

Arnadottir J, Chalfie M (2010) Eukaryotic mechanosensitive channels. Annu Rev Biophys 39:111-137.

Babu KS, Barth FG (1984) Neuroanatomy of the central nervous system of the wandering spider, *Cupiennius salei* (Arachnida, Araneida). 104:344-359.

Bae C, Sachs F, Gottlieb PA (2011) The mechanosensitive ion channel Piezo1 is inhibited by the peptide GsMTx4. Biochemistry 50:6295-6300.

Barth FG (2002) A spider's world: Senses and behavior. Heidelberg: Springer Verlag.

Barth FG (2004) Spider mechanoreceptors. Curr Opin Neurobiol 14:415-422.

Barth FG (2019) Mechanics to pre-process information for the fine tuning of mechanoreceptors J Comp Physiol A Doi: 10.1007/s00359-019-01355-z. [Epub ahead of print

Barth FG, Libera W (1970) Ein Atlas der Spaltsinnesorgane von *Cupiennius salei* Keys. Chelicerata (Aranea). Z Morphol Tiere 68:343-369.

Beurg M, Fettiplace R (2017) PIEZO2 as the anomalous mechanotransducer channel in auditory hair cells. J Physiol 595:7039-7048.

Bielefeldt K and Davis BM (2008) Differential effects of ASIC3 and TRPV1 deletion on gastroesophageal sensation in mice. Am J Physiol Gastrointest Liver Physiol 294:130-138.

Canessa CM, Schild L, Buell G, Thorens B, Gautschi I, Horisberger JD, Rossier BC (1994) Amiloride-sensitive epithelial Na^+ channel is made of three homologous subunits. Nature 367:463-467.

Chalfie M, Sulston J (1981) Developmental genetics of the mechanosensory neurons of *Caenorhabditis elegans*. Dev Biol 82:358-370.

Chalfie M, Driscoll M, Huang M (1993) Degenerin similarities. Nature 361:504

Cheng LE, Song W, Looger LL, Jan LY, Jan YN (2010) The role of the TRP channel NompC in *Drosophila* larval and adult locomotion. Neuron 67:373-380.

Contchart Software (2019) ControlFreak, control charts for individual data points. ControlFreak by Conchart Software, online at https://contchart.com/, accessed February-May, 2019.

Coste B, Mathur J, Schmidt M, Earley TJ, Ranade S, Petrus MJ, Dubin AE, Patapoutian A (2010) Piezo1 and Piezo2 are essential components of distinct mechanically activated cation channels. Science 330:55-60.

Coste B, Xiao B, Santos JS, Syeda R, Grandl J, Spencer KS, Kim SE, Schmidt M, Mathur J, Dubin AE, Montal M, Patapoutian A (2012) Piezo proteins are pore-forming subunits of mechanically activated channels. Nature 483:176-181.

Coste B, Murthy SE, Mathur J, Schmidt M, Mechioukhi Y, Delmas P, Patapoutian A (2015) Piezo1 ion channel pore properties are dictated by C-terminal region. Nat Commun 6:7223.

Cueva JG, Mulholland A, Goodman MB (2007) Nanoscale organization of the MEC-4 DEG/ENaC sensory mechanotransduction channel in *Caenorhabditis elegans* touch receptor neurons. J Neurosci 27:14089-14098.

Eberl DF, Hardy RW, Kernan MJ (2000) Genetically similar transduction mechanisms for touch and hearing in *Drosophila*. J Neurosci 20:5981-5988.

Effertz T, Wiek R, Gopfert MC (2011) NompC TRP channel is essential for Drosophila sound receptor function. Curr Biol 21:592-597.

Fabian-Fine R, Höger U, Seyfarth E-A, Meinertzhagen IA (1999) Peripheral synapses at identified mechanosensory neurons in spiders: Three-dimensional reconstruction and GABA-immunoreactivity. J Neurosci 19:298-310.

Fabian-Fine R, Seyfarth E-A, Meinertzhagen IA (2002) Peripheral synaptic contacts at mechanoreceptors in arachnids and crustaceans: Morphological and immunocytochemical characteristics. Microsc Res Tech 58:283-298.

Fabian-Fine R, Anderson CM, Roush MA, Johnson JAG, Liu H, French AS, Torkkeli PH (2017) The distribution of cholinergic neurons and their co-localization with FMRFamide, in central and peripheral neurons of the spider *Cupiennius salei*. Cell Tissue Res 370:71-88.

Fettiplace R (2017) Hair cell transduction, tuning, and synaptic transmission in the mammalian cochlea. Compr Physiol 7:1197-1227.

Fettiplace R, Kim KX (2014) The physiology of mechanoelectrical transduction channels in hearing. Physiol Rev 94:951-986.

French AS (1988) Transduction mechanisms of mechanosensilla. Annu Rev Entomol 33:39-58.

French AS (2012) Transcriptome walking: a laboratory-oriented GUI-based approach to mRNA identification from deep-sequenced data. BMC Res Notes 5:673-680

French AS, Torkkeli PH (2004) Mechanotransduction in spider slit sensilla. Can J Physiol Pharmacol 82:541-548.

French AS, Höger U, Sekizawa S-I, Torkkeli PH 2001: Frequency response functions and information capacities of paired mechanoreceptor neurons. Biol. Cybern. 85: 293-300.

French AS, Torkkeli PH, Seyfarth E-A (2002) From stress and strain to spikes: mechanotransduction in spider slit sensilla. J Comp Physiol A 188:739-752.

French AS, Meisner S, Liu H, Weckström M, Torkkeli PH (2015) Transcriptome analysis and RNA interference of cockroach phototransduction indicate three opsins and suggest a major role for TRPL channels. Front Physiol 6:207.

Ge J, Li W, Zhao Q, Li N, Chen M, Zhi P, Li R, Gao N, Xiao B, Yang M (2015) Architecture of the mammalian mechanosensitive Piezo1 channel. Nature 527:64- 69.

Gingl E, French AS (2003) Active signal conduction through the sensory dendrite of a spider mechanoreceptor neuron. J Neurosci 23:6096-6101.

Gingl E, French AS, Panek I, Meisner S, Torkkeli PH (2004) Dendritic excitability and localization of GABA-mediated inhibition in spider mechanoreceptor neurons. Eur J Neurosci 20:59-65.

Gnanasambandam R, Ghatak C, Yasmann A, Nishizawa K, Sachs F, Ladokhin AS, Sukharev SI, Suchyna TM (2017) GsMTx4: Mechanism of inhibiting mechanosensitive ion channels. Biophys J 112:31-45.

Gong J, Wang Q, Wang Z (2013) NOMPC is likely a key component of *Drosophila* mechanotransduction channels. Eur J Neurosci :.

Gong Z, Son W, Chung YD, Kim J, Shin DW, McClung CA, Lee Y, Lee HW, Chang DJ, Kaang BK, Cho H, Oh U, Hirsh J, Kernan MJ, Kim C (2004) Two interdependent TRPV channel subunits, inactive and Nanchung, mediate hearing in *Drosophila*. J Neurosci 24:9059-9066.

Goodman MB, Ernstrom GG, Chelur DS, O'Hagan R, Yao CA, Chalfie M (2002) MEC-2 regulates *C. elegans* DEG/ENaC channels needed for mechanosensation. Nature 415:1039-1042.

Göpfert MC, Albert JT, Nadrowski B, Kamikouchi A (2006) Specification of auditory sensitivity by *Drosophila* TRP channels. Nat Neurosci 9:998-1000.

Grünert U, Gnatzy W (1987) K^+ and Ca^{++} in the receptor lymph of arthropod cuticular mechanoreceptors. J Comp Physiol A 161:329-333.

Guo YR, MacKinnon R (2017) Structure-based membrane dome mechanism for Piezo mechanosensitivity. Elife 6: 10.

Hardie RC (2014) Photosensitive TRPs. Handb Exp Pharmacol 223:795-826.

Hennenfent A., Liu H., Torkkeli P.H. & French A.S 2019: RNA interference supports a role for Nanchung-Inactive in mechanotransduction by the cockroach, *Periplaneta americana* tactile spine. Submitted J. N

Höger U, French AS (1999) Estimated single-channel conductance of mechanically-activated channels in a spider mechanoreceptor. Brain Res 826:230-235.

Höger U, French AS (2002) Extracellular acid increases the open probability of transduction channels in spider mechanoreceptors. Eur J Neurosci 16:2311-2316.

Höger U, Torkkeli PH, Seyfarth E-A, French AS (1997) Ionic selectivity of mechanically activated channels in spider mechanoreceptor neurons. J Neurophysiol 78:2079-2085.

Holt JR, Pan B, Koussa MA, Asai Y (2014) TMC function in hair cell transduction. Hear Res 311:17-24

Juusola M, Seyfarth E-A, French AS (1994) Sodium-dependent receptor current in a new mechanoreceptor preparation. J Neurophysiol 72:3026-3028.

Kashlan OB, Kleyman TR (2011) ENaC structure and function in the wake of a resolved structure of a family member. Am J Physiol Renal Physiol 301:F684-F696.

Katta S, Krieg M, Goodman MB (2015) Feeling force: Physical and physiological principles enabling sensory mechanotransduction. Annu Rev Cell Dev Biol 31:347-371.

Kawashima Y, Géléoc GS, Kurima K, Labay V, Lelli A, Asai Y, Y, Makishima T, Wu DK, Della Santina CC, Holt JR, Griffith AJ. (2011) Mechanotransduction in mouse inner ear hair cells requires transmembrane channel-like genes. J Clin Invest 121, 4796–4809. doi: 10.1172/JCI60405

Keresztes G, Mutai H, Heller S (2003) TMC and EVER genes belong to a larger novel family, the TMC gene family encoding transmembrane proteins. BMC Genomics 4:24.

Kim J, Chung YD, Park DY, Choi S, Shin DW, Soh H, Lee HW, Son W, Yim J, Park CS, Kernan MJ, Kim C (2003) A TRPV family ion channel required for hearing in *Drosophila*. Nature 424:81-84.

Kim SE, Coste B, Chadha A, Cook B, Patapoutian A (2012) The role of *Drosophila* Piezo in mechanical nociception. Nature 483:209-212.

Klagges BR, Heimbeck G, Godenschwege TA, Hofbauer A, Pflugfelder GO, Reifegerste R, Reisch D, Schaupp M, Buchner S, Buchner E (1996) Invertebrate synapsins: a single gene codes for several isoforms in *Drosophila*. J Neurosci 16:3154-3165.

Lacroix JJ, Botello-Smith WM, Luo Y (2018) Probing the gating mechanism of the mechanosensitive channel Piezo1 with the small molecule Yoda1. Nat Commun 9:1-13.

Lee J, Moon S, Cha Y, Chung YD (2010) *Drosophila* TRPN(=NOMPC) channel localizes to the distal end of mechanosensory cilia. PLoS One 5:e11012.

Levin M (2004) A novel immunohistochemical method for evaluation of antibody specificity and detection of labile targets in biological tissue. J Biochem Biophys Methods 58:85-96.

Lewis AH. Cui AF, McDonald MF, Grandl J (2017) Transduction of repetitive mechanical stimuli by Piezo1 and Piezo2 ion channels. Cell Rep 19:2572-2585

Liang X, Madrid J, Gartner R, Verbavatz JM, Schiklenk C, Wilsch-Brauninger M, Bogdanova A, Stenger F, Voigt A, Howard J (2013) A NOMPC-dependent membrane-microtubule connector is a candidate for the gating spring in fly mechanoreceptors. Curr Biol 23:755-763.

Liu C, Montell C (2015) Forcing open TRP channels: Mechanical gating as a unifying activation mechanism. Biochem Biophys Res Commun 460:22-25.

Liu H, French AS, Torkkeli PH (2017) Expression of Cys-loop receptor subunits and acetylcholine binding protein in the mechanosensory neurons, glial cells and muscle tissue of the spider *Cupiennius salei*. J Comp Neurol 525:1139-1154.

Lowry R (2019) VassarStats: Website for Statistical Computation. Richard Lowry, online at http://vassarstats.net/, accessed February-May, 2019.

Malecot CO, Bito V, Argibay JA (1998) Ruthenium red as an effective blocker of calcium and sodium currents in guinea-pig isolated ventricular heart cells. Br J Pharmacol 124:465-472.

Murthy SE, Dubin AE, Patapoutian A (2017) Piezos thrive under pressure: mechanically activated ion channels in health and disease. Nat Rev Mol Cell Biol 18:771-783.

Nilius B, Honoré E (2012) Sensing pressure with ion channels. Trends Neurosci 35:477-486.

O'Hagan R, Chalfie M, Goodman MB (2005) The MEC-4 DEG/ENaC channel of *Caenorhabditis elegans* touch receptor neurons transduces mechanical signals. Nat Neurosci 8:43-50.

Omerbasic D, Schuhmacher L, Bernal Sierra Y, St John Smith E, Lewin GR (2014) ASICs and mammalian mechanoreceptor function. Neuropharmacology 94:80-86

Owsianik G, Talavera K, Voets T, Nilius B (2006) Permeation and selectivity of TRP channels. Annu Rev Physiol 68:685-717.

Paluch EK, Nelson CM, Biais N, Fabry B, Moeller J,. Pruitt BL, Wollnik C, Kudryasheva G, Rehfeldt F, Federle W (2015) Mechanotransduction: use the force(s). BMC Biology 13:47. DOI: 10.1186/s12915-015-0150-4.

Pan B, Akyuz N, Liu XP, Asai Y, Nist-Lund C, Kurima K, Derfler BH, Gyorgy B, Limapichat W, Walujkar S, Wimalasena LN, Sotomayor M, Corey DP, Holt JR (2018) TMC1 forms the pore of mechanosensory transduction channels in vertebrate inner ear hair cells. Neuron 99:736-753.

Panek I, French AS, Seyfarth E-A, Sekizawa S-i, Torkkeli PH (2002) Peripheral GABAergic inhibition of spider mechanosensory afferents. Eur J Neurosci 16:96-104.

Panek I, Höger U, French AS, Torkkeli PH (2008) Contributions of voltage- and Ca^{2+}-activated conductances to GABA induced depolarization in spider mechanosensory neurons. J Neurophysiol 99:1596-1606.

Parpaite T, Coste B (2017) Piezo channels. Curr Biol 27:R250-R252.

Pfeiffer K, Panek I, Höger U, French AS, Torkkeli PH (2009) Random stimulation of spider mechanosensory neurons reveals long-lasting excitation by GABA and muscimol. J Neurophysiol 101:54-66.

Piacentini LN, Ramirez MJ (2019) Hunting the wolf: A molecular phylogeny of the wolf spiders (Araneae, Lycosidae). Mol Phylogenet Evol 136:227-240.

Price MP, McIlwrath SL, Xie J, Cheng C, Qiao J, Tarr DE, Sluka KA, Brennan TJ, Lewin GR, Welsh MJ (2001) The DRASIC cation channel contributes to the detection of cutaneous touch and acid stimuli in mice. Neuron 32:1071-1083.

Qiu X, Müller U (2018) Mechanically gated ion channels in mammalian hair cells. Front Cell Neurosci 12:100.

Saari P, French AS, Torkkeli PH, Liu H, Immonen EV, Frolov RV (2017) Distinct roles of light-activated channels TRP and TRPL in photoreceptors of *Periplaneta americana*. J Gen Physiol 149:455-464.

Scheffer DI, Shen J, Corey DP, Chen ZY (2015) Gene expression by mouse inner ear hair cells during development. J Neurosci 35, 6366–6380.

Sekizawa S-i, French AS, Höger U, Torkkeli PH (1999) Voltage-activated potassium outward currents in two types of spider mechanoreceptor neurons. J Neurophysiol 81:2937-2944.

Seyfarth E-A, French AS (1994) Intracellular characterization of identified sensory cells in a new spider mechanoreceptor preparation. J Neurophysiol 71:1422-1427.

Seyfarth E-A, Sanders EJ, French AS (1995) Sodium channel distribution in a spider mechanosensory organ. Brain Res 683:93-101.

Simon A, Shenton FC, Hunter I, Banks RW, Bewick GS (2010) Amiloride-sensitive channels are a major contributor to mechanotransduction in mammalian muscle. J Physiol 588:171-185.

Suchyna TM (2017) Piezo channels and GsMTx4: Two milestones in our understanding of excitatory mechanosensitive channels and their role in pathology. Prog Biophys Mol Biol 130:244-253.

Sukumar V, Liu H, Meisner S, French AS, Torkkeli PH (2018) Multiple biogenic amine receptor types modulate spider, *Cupiennius salei*, mechanosensory neurons. Front Physiol 9:857.

Suslak TJ, Watson S, Thompson KJ, Shenton FC, Bewick GS, Armstrong JD, Jarman AP (2015) Piezo is essential for amiloride-sensitive stretch-activated mechanotransduction in larval *Drosophila* dorsal bipolar dendritic sensory neurons. PLoS One 10:e0130969.

Syeda R, Xu J, Dubin AE, Coste B, Mathur J, Huynh T, Matzen J, Lao J, Tully DC, Engels IH, Petrassi HM, Schumacher AM, Montal M, Bandell M, Patapoutian A (2015) Chemical activation of the mechanotransduction channel Piezo1. Elife 4: 10.

Torkkeli PH, French AS (1994) Characterization of a transient outward current in a rapidly adapting insect mechanosensory neuron. Pflügers Arch 429:72-78.

Torkkeli PH, Liu H, French AS (2015) Transcriptome analysis of the central and peripheral nervous systems of the spider *Cupiennius salei* reveals multiple putative Cys-loop ligand gated ion channel subunits and an acetylcholine binding protein. PLoS One 10:e0138068.

Torkkeli P.H., Johnson J.A.G., Liu H., Sivapalan K. & French A.S. 2018: Is Piezo protein the mechanotransduction channel in spider *Cupiennius salei* mechanosensilla? 13th International Congress of Neuroethology.

von Trotha JW, Vernier P, Bally-Cuif L (2014) Emotions and motivated behavior converge on an amygdala-like structure in the zebrafish. Eur J Neurosci 40:3302-3315.

Walder RY, Rasmussen LA, Rainier JD, Light AR, Wemmie JA, Sluka KA (2010) ASIC1 and ASIC3 play different roles in the development of hyperalgesia after inflammatory muscle injury. J Pain Off J Am Pain Soc 11:210-218.

Walker RG, Willingham AT, Zuker CS (2000) A *Drosophila* mechanosensory transduction channel. Science 287:2229-2234.

Wang Z, Gerstein M, Snyder M (2009) RNA-Seq: a revolutionary tool for transcriptomics. Nat Rev Genet 10:57-63.

Warren B, Matheson T (2018) The role of the mechanotransduction ion channel candidate Nanchung-Inactive in auditory transduction in an insect ear. J Neurosci 38:3741-3752.

Widmer A, Höger U, Meisner S, French AS, Torkkeli PH (2005) Spider peripheral mechanosensory neurons are directly innervated and modulated by octopaminergic efferents. J Neurosci 25:1588-1598.

World Spider Catalog (2019). World Spider Catalog. Version 20.0. Natural History Museum Bern, online at http://wsc.nmbe.ch, accessed on May 30th, 2019, doi: 10.24436/2

Zhao Q, Zhou H, Chi S, Wang Y, Wang J, Geng J, Wu K, Liu W, Zhang T, Dong MQ, Wang J, Li X, Xiao B (2018) Structure and mechanogating mechanism of the Piezo1 channel. Nature 554:487-492.

APPENDIX 1. Primer sequences used for generation of RNA probes for in-situ hybridization.

Name/ID	Accession No.	Antisense Primers	Sense Primers
Piezo/0288	GAKT01000106	**F:**GCAATGGAGTAGACTTCAAACTGCTG **R:**TAATACGACTCACTATAGGGAGCACTCTATCCACGTATGGCATATC	**F:**TAATACGACTCACTATAGGGGCAATGGAGTAGACTTCAAACTGCTG **R:**AGCACTCTATCCACGTATGGCATATC
Tmc-7/0368	GBFC01000027	**F:**ACTGTAATAGAAGCCGGTCATGC **R:**TAATACGACTCACTATAGGGCTCTTGCTTGAATAGGGCACATC	**F:**TAATACGACTCACTATAGGGACTGTAATAGAAGCCGGTCATGC **R:**CTCTTGCTTGAATAGGGCACATC
Tmc-5/0369	GBFC01000028	**F:**GATCCTGGTCTGTGAATGAGGC **R:**TAATACGACTCACTATAGGGCCAGGCTGATGAGAAGGTATCAG	**F:**TAATACGACTCACTATAGGGGATCCTGGTCTGTGAATGAGGC **R:**CCAGGCTGATGAGAAGGTATCAG
Amil-1/0477	N/A	**F:**CATCTTCTGCCGTCTCCTTATC **R:**TAATACGACTCACTATAGGGGTCTTCGATAGCCATTCTTCCTAC	**F:**TAATACGACTCACTATAGGGCATCTTCTGCCGTCTCCTTATC **R:**GTCTTCGATAGCCATTCTTCCTAC
Amil-2/0449	N/A	**F:**TTCACAGCTTGTAACATCCAGTG **R:**TAATACGACTCACTATAGGGAGCTCACCTGATTTCTTTCCG	**F:**TAATACGACTCACTATAGGGTTCACAGCTTGTAACATCCAGTG **R:**AGCTCACCTGATTTCTTTCCG
Trp-1/0283	GAKT01000102	**F:**GTATTGCGACGCACTGTATAGCC **R:**TAATACGACTCACTATAGGGCTTCTTGTGACTCGTCTCTGCCA	**F:**TAATACGACTCACTATAGGGGTATTGCGACGCACTGTATAGCC **R:**CTTCTTGTGACTCGTCTCTGCCA
Trp-2/0478	N/A	**F:**TGATGTCGATGAAGACCTTCAGCAG	**F:**TAATACGACTCACTATAGGGTGATGTC

Name/ID	Accession No.	Antisense Primers	Sense Primers
		R:TAATACGACTCACTATAGGGCTAACTGCAATACAGCAGCTCTCTCG	GATGAAGACCTTCAGCAG **R:**CTAACTGCAATACAGCAGCTCTCTCG
Deg-1/285	GAKT01000103	**F:**CCAATGCTCAGCCTTATACGACTG **R:**TAATACGACTCACTATAGGGCTCCATTTCAAGCACCATGTG	**F:**TAATACGACTCACTATAGGCCAATGCTCAGCCTTATACGACTG **R:**GCTCCATTTCAAGCACCATGTG
Deg-2/287	GAKT01000105	**F:**TACTACTGCGACGGAAACAGGTCC **R:**TAATACGACTCACTATAGGGAACGACAGCCCTCAAGTAGTTCCTC	**F:**TAATACGACTCACTATAGGGTACTACTGCGACGGAAACAGGTCC **R:**AACGACAGCCCTCAAGTAGTTCCTC

Accession No. = GenBank accession number; ID = identification # in the laboratory; TMC = Transmembrane channel; Amil = Amiloride sensitive ion channel; TRP = Transient receptor potential channel; Deg = Epithelial sodium channel (ENaC) in Degenerin family; F = forward polarity, R = reverse polarity.

APPENDIX 2. Springer Nature Copyright Permission for Figure 1.2.

SPRINGER NATURE LICENSE
TERMS AND CONDITIONS

Jun 03, 2019

This Agreement between Dalhousie University -- Jessica Johnson ("You") and Springer Nature ("Springer Nature") consists of your license details and the terms and conditions provided by Springer Nature and Copyright Clearance Center.

License Number	4599420620342
License date	May 31, 2019
Licensed Content Publisher	Springer Nature
Licensed Content Publication	Cell and Tissue Research
Licensed Content Title	The distribution of cholinergic neurons and their co-localization with FMRFamide, in central and peripheral neurons of the spider Cupiennius salei
Licensed Content Author	Ruth Fabian-Fine, Carly M. Anderson, Molly A. Roush et al
Licensed Content Date	Jan 1, 2017
Licensed Content Volume	370
Licensed Content Issue	1
Type of Use	Thesis/Dissertation
Requestor type	academic/university or research institute
Format	print and electronic
Portion	figures/tables/illustrations
Number of figures/tables/illustrations	1
Will you be translating?	no
Circulation/distribution	<501
Author of this Springer Nature content	yes
Title	Molecules involved in the spider, Cupiennius salei, mechanotransduction
Institution name	Dalhousie University
Expected presentation date	Jul 2019
Order reference number	1
Portions	Figure 1
Requestor Location	Dalhousie University PO BOX 15000 Halifax, NS B3H 4R2 Canada Attn: Dalhousie University

Total 0.00 USD

Terms and Conditions

Springer Nature Terms and Conditions for RightsLink Permissions

Springer Nature Customer Service Centre GmbH (the Licensor) hereby grants you a non-exclusive, world-wide licence to reproduce the material and for the purpose and requirements specified in the attached copy of your order form, and for no other use, subject to the conditions below:

1. The Licensor warrants that it has, to the best of its knowledge, the rights to license reuse of this material. However, you should ensure that the material you are requesting is original to the Licensor and does not carry the copyright of another entity (as credited in the published version).

   If the credit line on any part of the material you have requested indicates that it was reprinted or adapted with permission from another source, then you should also seek permission from that source to reuse the material.

2. Where **print only** permission has been granted for a fee, separate permission must be obtained for any additional electronic re-use.

3. Permission granted **free of charge** for material in print is also usually granted for any electronic version of that work, provided that the material is incidental to your work as a whole and that the electronic version is essentially equivalent to, or substitutes for, the print version.

4. A licence for 'post on a website' is valid for 12 months from the licence date. This licence does not cover use of full text articles on websites.

5. Where **'reuse in a dissertation/thesis'** has been selected the following terms apply: Print rights of the final author's accepted manuscript (for clarity, NOT the published version) for up to 100 copies, electronic rights for use only on a personal website or institutional repository as defined by the Sherpa guideline (www.sherpa.ac.uk/romeo/).

6. Permission granted for books and journals is granted for the lifetime of the first edition and does not apply to second and subsequent editions (except where the first edition permission was granted free of charge or for signatories to the STM Permissions Guidelines http://www.stm-assoc.org/copyright-legal-affairs/permissions/permissions-guidelines/), and does not apply for editions in other languages unless additional translation rights have been granted separately in the licence.

7. Rights for additional components such as custom editions and derivatives require additional permission and may be subject to an additional fee. Please apply to Journalpermissions@springernature.com/bookpermissions@springernature.com for these rights.

8. The Licensor's permission must be acknowledged next to the licensed material in print. In electronic form, this acknowledgement must be visible at the same time as the figures/tables/illustrations or abstract, and must be hyperlinked to the journal/book's homepage. Our required acknowledgement format is in the Appendix below.

9. Use of the material for incidental promotional use, minor editing privileges (this does not include cropping, adapting, omitting material or any other changes that affect the meaning, intention or moral rights of the author) and copies for the disabled are permitted under this licence.

10. Minor adaptations of single figures (changes of format, colour and style) do not require the Licensor's approval. However, the adaptation should be credited as shown in Appendix below.

Appendix — Acknowledgements:

For Journal Content:
Reprinted by permission from [**the Licensor**]: [**Journal Publisher** (e.g. Nature/Springer/Palgrave)] [**JOURNAL NAME**] [**REFERENCE CITATION** (Article name, Author(s) Name), [**COPYRIGHT**] (year of publication)

For **Advance Online Publication papers:**
Reprinted by permission from [**the Licensor**]: [**Journal Publisher** (e.g. Nature/Springer/Palgrave)] [**JOURNAL NAME**] [**REFERENCE CITATION** (Article name, Author(s) Name), [**COPYRIGHT**] (year of publication), advance online publication, day month year (doi: 10.1038/sj.[JOURNAL ACRONYM].)

For Adaptations/Translations:
Adapted/Translated by permission from [**the Licensor**]: [**Journal Publisher** (e.g. Nature/Springer/Palgrave)] [**JOURNAL NAME**] [**REFERENCE CITATION** (Article name, Author(s) Name), [**COPYRIGHT**] (year of publication)

Note: For any republication from the British Journal of Cancer, the following credit line style applies:

Reprinted/adapted/translated by permission from [**the Licensor**]: on behalf of Cancer Research UK: : [**Journal Publisher** (e.g. Nature/Springer/Palgrave)] [**JOURNAL NAME**] [**REFERENCE CITATION** (Article name, Author(s) Name), [**COPYRIGHT]** (year of publication)

For **Advance Online Publication** papers:
Reprinted by permission from The [**the Licensor**]: on

behalf of Cancer Research UK: [**Journal Publisher** (e.g. Nature/Springer/Palgrave)] [**JOURNAL NAME**] [**REFERENCE CITATION** (Article name, Author(s) Name), [**COPYRIGHT**] (year of publication), advance online publication, day month year (doi: 10.1038/sj. [JOURNAL ACRONYM])

For Book content:
Reprinted/adapted by permission from [**the Licensor**]: [**Book Publisher** (e.g. Palgrave Macmillan, Springer etc) [**Book Title**] by [**Book author**(s)] [**COPYRIGHT**] (year of publication)

Other Conditions:

Version 1.1